System Design and Evaluation of a Low Cost Epidural Intracranial Pressure Monitoring System, Integrable with ECoG Electrodes

by

Ranjani Sampath Kumaran

A Thesis Presented in Partial Fulfillment
of the Requirements for the Degree
Master of Science

Approved April 2015 by the
Graduate Supervisory Committee:

Jennifer Blain Christen, Chair
Bradley Greger
Stephen Helms Tillery

ARIZONA STATE UNIVERSITY

May 2015

ABSTRACT

Intracranial pressure is an important parameter to monitor, and elevated intracranial pressure can be life threatening. Elevated intracranial pressure is indicative of distress in the brain attributed by conditions such as aneurysm, traumatic brain injury, brain tumor, hydrocephalus, stroke, or meningitis.

Electrocorticography (ECoG) recordings are invaluable in understanding epilepsy and detecting seizure zones. However, ECoG electrodes cause a foreign body mass effect, swelling, and pneumocephaly, which results in elevation of intracranial pressure (ICP).Thus, the aim of this work is to design an intracranial pressure monitoring system that could augment ECoG electrodes.

A minimally invasive, low-cost epidural intracranial pressure monitoring system is developed for this purpose, using a commercial pressure transducer available for biomedical applications. The system is composed of a pressure transducer, sensing cup, electronics, and data acquisition system. The pressure transducer is a microelectromechanical system (MEMS)-based die that works on piezoresistive phenomenon with dielectric isolation for direct contact with fluids.

The developed system was bench tested and verified in an animal model to confirm the efficacy of the system for intracranial pressure monitoring. The system has a 0.1 mmHg accuracy and a 2% error for the 0-10 mmHg range, with resolution of 0.01 mmHg. This system serves as a minimally invasive (2 mm burr hole) epidural ICP

monitor, which could augment existing ECoG electrode arrays, to simultaneously measure intracranial pressure along with the neural signals.

This device could also be employed with brain implants that causes elevation in ICP due to tissue - implant interaction often leading to edema. This research explores the concept and feasibility for integrating the sensing component directly on to the ECoG electrode array.

DEDICATION

This is dedicated to my parents,

who believed in me and sponsored my education, compromising on their living.

I truly owe this to Him and Her, who has given life to me.

I did it!

ACKNOWLEDGMENTS

There are so many people that I am thankful for through my entire journey contained in these pages. First, I would like to thank Dr. Jennifer Blain Christen, committee chair, for all the support, help and guidance in completing this thesis. I thank her for believing in me more than I did myself throughout this work and for motivating when I needed the most. I am grateful to her for being very supportive through my worst stages of my life and for letting me work on my pace independently. I owe her a special mention for sponsoring this thesis work. If I would take something from her that would be "Being humble and keeping your feet on the ground, no matter what positions you hold in life"

Next, I'd like to thank Dr. Bradley Greger, my subject professor and committee member who has kindled that thought in me for researching on such a novel topic. He is a super positive person to work with and has clearly guided me on making innovative ideas into a tangible work. Special thanks to him for helping me with physiological part, animal testing involved in this work and for constant encouragement throughout.The list of talented mentors would not be complete without Dr. Stephen Helms Tillery who has been a great support throughout my Masters research. From the day I started my Masters, he has taught me what research is. He was the best graduate advisor in helping me figure out what I really wanted to do in life and also in understanding the difference between passion and interest with respect to work.

Not always a work is complete without those editors in back stage who chisel the art; I must thank this wonderful person - Zoe Browning, who has been a great help and support in drafting IACUC protocol, in defining surgical process and helping perform the

surgery at the last minute for wrapping up my thesis. I can't thank her enough. I also thank Rachele McAndrew a lot for all the help with surgery preparation.

I would like to extend my gratitude to my lab mates - Joseph Smith, Sashi, Dixy and Tao for all the help. A special mention to my friend and lab mate Krishna, without whom I could not have worked out my thesis this well. He is someone who taught me "You can never solve a problem from a state of Panic - you can only solve it from a state of Conviction". Thanks a ton for all the days you stayed back late in the night, helping me fix and figure out things in lab.I would like to thank my part time colleagues, who were constant source of encouragement - Veronica, whom I call my US mother, I'm blessed to have met her; Cathy, a bundle of positivity, and Mary Lou, who has always motivated me, appreciating for what I am. Thanks to PTS team at ASU.

Here goes thanks to best of my friends Raghu and Swarnima, who had been there to back me up for anything and everything! I definitely have to thank Krithi, the sister that I never had for all the things she has helped me with. Yash, my bestie not to be thanked. Ragav, who has instilled the thought in me for doing research. Arkadeep who has always told me "You didn't come here to say you can't do it" and a big thanks to Raj Anoosh, without whom I would never have applied for master. Also, special thanks to Sanchit Chirania, who has always wished the best for me and encouraged me in my worst times saying "Put your heart into what you do - it will never let you fail.I'm grateful to Laura Hawes for her support and constant reminder for all the deadlines during my master's studies, without whom I wouldn't have made it.When things don't go right, certain don't walk out and thanks is a simple word to say to them - Special thanks to my parents, friends and family for all the support and source of encouragement.

TABLE OF CONTENTS

LIST OF TABLES

LIST OF FIGURES

CHAPTER 1

INTRODUCTION

Intracranial Pressure

Intracranial pressure (ICP), commonly referred to as brain pressure, is the pressure inside the skull. Monitoring of intracranial pressure has been important in both neurosurgery and neurology for over two decades.

Head injury, brain swelling, tumors, and stroke are some of the most common brain related issues that leads to or are associated with increase in brain pressure. For example, Traumatic Brain Injury (TBI), usually referred to as a head injury, is a devastating medical problem that has huge socioeconomic consequence. There are about 52,000 deaths and 275,000 hospitalizations every year due to TBI in the USA[1]. Currently, there are both invasive and noninvasive ICP monitoring technologies on the market. However, direct or fully-invasive measurement and detection of ICP remains the standard, especially for brain swelling or edema after an injury.

Invasive ICP monitors come with tradeoffs of having to deal with infection and postoperative complications. Thus we recognize there are disadvantages in fully-invasive system to be weighed against their excellent accuracy in determining the intracranial pressure. Noninvasive techniques are, of course, preferable with regard to infections and complications, but they haven't been used clinically to a great extent due to inaccuracies resulting from correlation or calibration factors involved[2,3,4]. Given the aforementioned tradeoffs between fully-invasive and noninvasive systems there is a need for a minimally-invasive, highly accurate diagnostic tool that would monitor brain pressure.

There are several types of invasive ICP monitors currently available. They are classified based on the location of the device or sensor inside the skull, which relates to the rate of infection and postoperative complications. The location of the sensor inside the skull determines the size of craniotomy (burr hole on the skull) required, which in turn is linked with the infection rate. Examining these monitoring configurations along with their benefits and complications, provide us insight into the design of an ICP monitor that fulfills the unmet clinical need.

Problem Statement

In examining neural technologies, we observe the enormous importance of monitoring to provide insight into how the brain works. One of the most important type of monitors examines patterns of electrical activity in the brain; this is called electrocorticography.

Electrocorticography (ECoG), often referred to as intracranial electroencephalogram (EEG), is a method of recording neural potentials through placement of electrodes on the surface of the brain. This is an incredibly useful tool for understanding the brain and providing therapies for numerous diseases. For instance, this procedure is specifically performed to understand the epileptic foci in brain that causes seizures, which can be removed by a surgery. There are two kinds of ECoG:

1) Intraoperative - electrodes are placed during a lesion removal surgery to map the epileptic zones before surgery and are removed after surgery

2) Extraoperative - electrodes are placed for a short term implantation of 4-5 days to evaluate and map the brain activity over the area of epileptic foci and then removed. This is generally used to get a better understanding of the foci before the surgery.

Both require surgery and placement is in subdural space, with continuous monitoring. There are three kinds of electrodes in use - strip, grid and depth electrodes. Strip electrode are used for small areas, grid for a larger areas and depth for investigating deep brain structures such as the amygdala and the hippocampus. Any surgical procedure involves risks of infection and other complications. One of the major risk includes cerebral edema or brain swelling due to the presence of the electrode, and if the swelling is extreme a secondary surgery is performed to remove the electrodes.

The recent developments in understanding epilepsy have given birth to design of the wireless, implantable ECoG (electrocorticography) electrode system, which is used to monitor epileptic seizure zones in brain. Further, advancements in Brain Machine Interface (BMI) have also lead to wireless ECoG system design[5-8]. However, an important parameter often overlooked is the feedback from changes occurring during an implantation of such a system over time (e.g. 5 day recordings). In the case of surgery and implantation, some level of edema always occurs. Hence, we need a monitor to provide feedback on the level of edema. This strongly indicates the need for pressure measurement integration with the wireless ECoG development[9,10].

Looking at the currently available microtransducers, we find none of them are exactly suitable for our purpose, integration on the ECoG electrodes. The microtransducers available use various sensing technologies such as piezoresistors, fiber optics, fluid filled

strain gauge tip catheter, etc. All the existing clinically approved commercial devices are wired, having a catheter or some extension for the sensor to be placed in the brain. Further, dimensionally the existing systems are unsuitable for integration. Beyond, the commercially existing microtransducers cost $400-$600, just for the sensor and excluding surgical, monitoring, and surgeon fees. This has lead us to attempt to find a cost effective solution for an ICP monitoring device that could be integrated with ECoG electrodes.

Goals of this Research work:

The goal was to find a simple, cost-effective, and miniaturized pressure transducer that could be integrated with the developing wireless ECoG arrays. This indicates we need a pressure sensitive material or layer that could be embed onto the ECoG grid.

The specific goals of this thesis work are:

1) To find a pressure transducer material that could potentially be integrated with ECoG grid electrodes- determine dimensions and affordability match

2) To calibrate and evaluate the transducer to obtain a proof of concept that the system could potentially work well in measuring intracranial pressure.

Contribution of this thesis to solve the novel problem:

Piezoresistive technology was chosen as the focus of research considering the frequency characteristics of the ICP signal. Piezoresistance is a phenomenon of change in resistance of a material when a mechanical stress is applied. Unlike piezorelectricity, this

phenomenon is an active transducing system meaning itrequires energy to convert the pressure changes to a resistance or voltage changes.

First, force resistive sensors (FSR) were investigated, which are usually used to detect high pressure. The sensing layer was modified for our application at a lower range of pressures, which hadn't previously been tested for these devices to our knowledge.

Additionally, a commercial disposable blood pressure sensor was investigated to measure intracranial pressure. This sensor has a Micro-ElectroMechanical System (MEMS) die within that detects the changes in pressure. This die is available commercially and used in medical devices, which is helpful for furthering this research to integrate the die on the ECoG system and evaluating it.

CHAPTER 2

BACKGROUND

Anatomical Locations for ICP Monitoring:

The brain is enveloped by three protective membranes, collectively called the meninges. From the cranium towards the brain, the layers are dura mater, arachnoid mater and the pia mater. Cerebral pressure monitoring could be performed at five anatomically different locations namely ventricles or cavities in brain where CSF is produced; brain parenchyma (brain mass); below arachnoid mater (subarachnoid); below dura (subdural) and just below skull (epidural). ICP monitors based on these locations are categorized into two broad sectors:

1) Intra-ventricular catheter or External ventricular drainage (EVD)

2) Micro-transducers

The picture below describes the anatomical locations for ICP monitoring, where devices other than intra-ventricular catheter falls under micro-transducers category.

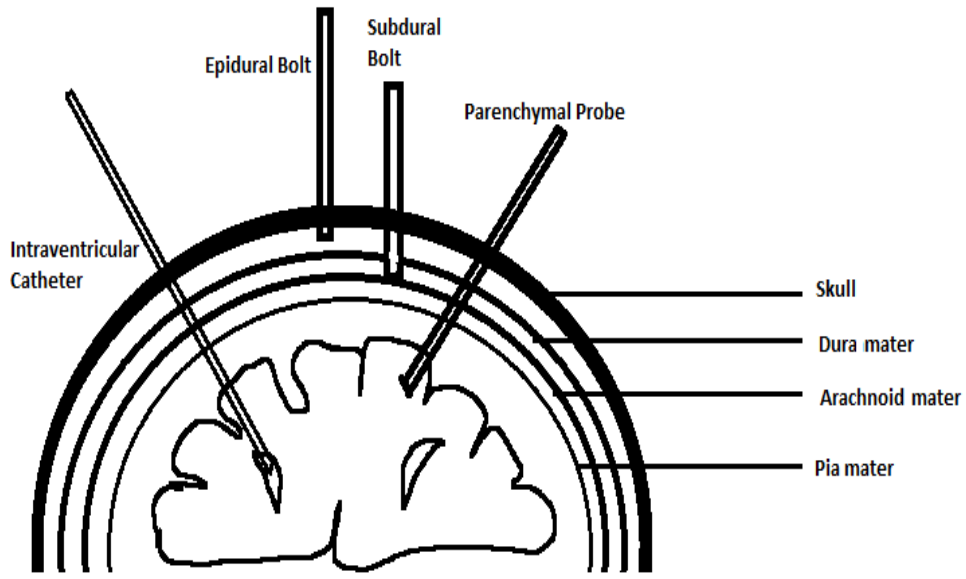

Figure 1. Anatomical locations for ICP Monitoring
This figure shows device placement area and the respective nomenclature.

Current and Existing Methods to Monitor ICP:

Intracranial pressure monitors are classified into invasive and non-invasive monitors. The invasive ICP devices are divided further as discussed above. In addition to these, ICP can be monitored invasively through a lumbar puncture technique by a spinal tap[11,12,13].

Invasive Intracranial Pressure Monitoring devices:

1) External Ventricular Drainage (EVD):

Intra-ventricular catheterization is considered the "gold standard" method for monitoring ICP. This is due to the precision and accuracy the measurement carries based

on the placement of the sensing area at the origin of CSF production. EVD has two main advantages over the other methods, which has high clinical significance:

i. Provides a way to drain the CSF to control elevated pressures
ii. Administer antibiotics for ventriculities or other infections that results from the EVD placement itself[14-18].

In this technique a catheter is placed on the lateral ventricle of the brain through a right frontal burr hole procedure. Usually, a coronal drill at Kocher's point is performed to position the tip of the catheter in the 3rd ventricle. Alternatively, other burr holes at Keen's point (posterior-parietal), Frazier's point (occipital-parietal) and Dandy's point (occipital) are also used to reach various ventricles as desired by the surgeon based on the clinical relevance[2].

The technology behind EVD to measure is either saline manometer or a pressure transducer, which is in contact with the drained CSF through a three way stop valve[3].The auditory meatus serves as an external reference for the transducer to be closely positioned to the center of the head or the foramen of Monro. Unfortunately, every time the head position is changed the transducers need repositioning.

Potential complications of this system include progressive edema due to infection or bacterial colonization that results in the ventricular system and compression or even blockage of the catheter drainage [2]. Further, EVDs are known for associated postoperative hemorrhages. On an average, 41% of the cases had post-traumatic hemorrhage in a study with 188 patients who underwent EVD catheterization, out of which 10.6 % are clinically significant or relevant having a neurological

deficit[19].Additionally, catheterization and placement for younger patients is still a problem due to a very slender ventricular system[2].

Bacterial or other infections due to EVDs range from 0-27% of the cases. If EVD treatment is used for longer than five days, the infection rate is further increased with other associated problems such as cranial fracture with CSF leakage, resulting in non-sterile EVD[20 - 23]. Infection rates are also increased by improper placement of the catheter resulting in damage to the parenchyma, penetrating the ventricles and other cerebral structures. In a patient population of 138 about 12.3% had misplaced catheters and higher infection rates[24]. It is recommended practice to use a "Ghajar guide" to correctly position the catheter rather than by hand, but according to a survey only 3% American neurosurgeons use this guide on a regular basis[25, 26]. Ventricular catheter misplacement rate is 6.3% which results in blockage of brain matter or blood clots[27, 28].This system is still very much in use in the clinical settings due to its ability to provide CSF drain to relieve pressure when intracranial hypertension is attributed by an abnormal mass[2].

2) Micro-transducers

Micro-transducer classifications are based on the technology used in the system to quantify the pressure. The various microtransducers in use are:

i. Fiber optic sensor - Camino
ii. Piezoresistive sensors - Codman, Raumedic and Pressio
iii. Pneumatic sensors - Spiegelberg

(i) The Camino ICP monitor is based on fiber optics principles, where the sensor transmits light via a fiber optic cable towards a displaceable mirror in contact with the brain tissues. The changes in the ICP are tracked through the difference in intensities between incident and reflected light. The sensor is usually placed in the intraparenchymal cells on the right frontal region about 2 cm deep. Placement over the brain parenchyma could be modified based on the pressure gradient suspected. Camino has different models for ventricular, parenchymal, subdural and epidural measurements[64]

Camino also has epidural ICP sensor models, but it does not provide the desired accuracy for regular clinical use. This is due to overestimation of ICP with a mean of 9 mmHg, extending up to 30 mmHg[29]. Despite large differencesin mean ICP values depending on placement, ICP waveform characteristics (pulse amplitude and wave time) still seemed comparable irrespective of the positions[30]. Studies show that above 20 mmHg, ICP measured epidurally is consistent with subdural measures[31]. Another study found out that subdural ICP recordings have excellent correlation with the ICP obtained from the lumbar puncture technique, proving that locations other than the ventricles or brain parenchyma can be used for ICP measurement[32]. This study also conclude that difference in epidural measures compare to other locations arise from the significant physiological pressure difference in compartments and not due to the monitoring systems themselves.

In a clinical study with a population of 1000 patients, 574 probes were investigated and 8.5% showed positive bacterial growth, 2.5% had incidences of hemorrhage (4 parenchymal and 2 epidural) and technical errors occurred in 4.5% of the

cases[33]. In another study with 328 patients, 1.1% cases had hemorrhage, 4.75% had infection and 3.14% cases were reported with technical errors or faulty sensors[34].

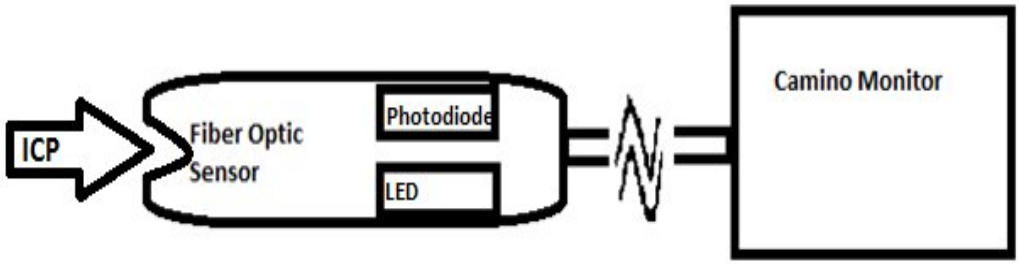

Figure 2. Construction of Camino sensor, adapted from Camino website [64]

(ii) *Codman MicroSensor* uses a microchip at the tip of the nylon tube that transduce the ICP changes in terms of resistance values that are reflected as voltage changes. Codman makes sensors for ventricular, parenchymal and subdural measurements[65]. Most of these are used for intraparenchymal placement with a 4mm burr hole and screw[3]. These sensors are considered almost as accurate as ventricular ICP measurements with very low infection and hemorrhages rates[35, 3]. Particularly when ventricles are inaccessible due to compression, Codman sensors are highly preferred[3]. In a clinical study of 1000 patients only 3 were found to have postoperative hemorrhages and no infection related to placement of the sensors were detected [36].

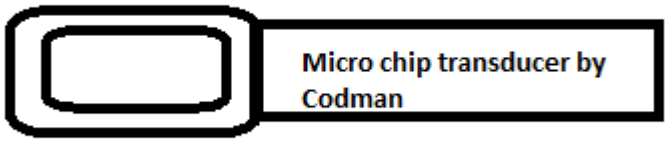

Figure 3. Construction of Codman sensor, adapted from Codman website [65]

Raumedic Neurovent-P sensor works on the same principle of resistance changes to monitor ICP. A study of 99 patients shows that Neurovent sensors have no or very low infection rates with only 2 cases of hemorrhage that required no intervention[37].

The Pressio ICP monitor also uses piezoresistive technology to measure ICP changes. This sensor has undergone vast bench and laboratory testing but hasn't been tested in vivo thoroughly yet. Studies by Lescot et al, demonstrated ICP measurements of 15 Pressio sensors in comparison with Codman sensors indicated a mean difference of ±7 mmHg between the recordings from two sensors [38]. We emphasized here that no complications such as infection or postoperative hemorrhage were evaluated or recorded. In laboratory evaluation of Pressio sensor the drift was less than 0.05 mmHg with accuracy 0.5 mmHg over 0-100 mmHg range of measure. Pulse waveform accuracy of Pressio sensor was 0.2 mmHg which is better than the Codman transducer in 0-20 mmHg range[39]

(iii) The S*piegelberg sensor* uses direct pneumatic changes to monitor ICP. This system has a small balloon at the distal end of a catheter to register the pressure changes and along with pressure this sensor can measure intracranial compliance. The Spiegelberg sensor has different models for ventricular, parenchymal and epidural measurement[66].

Lang et al[40] has tested this sensor in 87 patients and found no significant hemorrhage or clinical signs of meningitis, but 3 patients had faulty measurements due to a leaking issue with the sensor tip. When tested for continuous intracranial compliance (cICC) measures by Kiening et al[41], it seemed to have poor data quality, poor prediction with respect to ICP and correlation to cerebral hypoxia. However, later studies with respect to this sensor showed that these results in TBI might be due to age related decrease in compliance that shadowed the results[42].

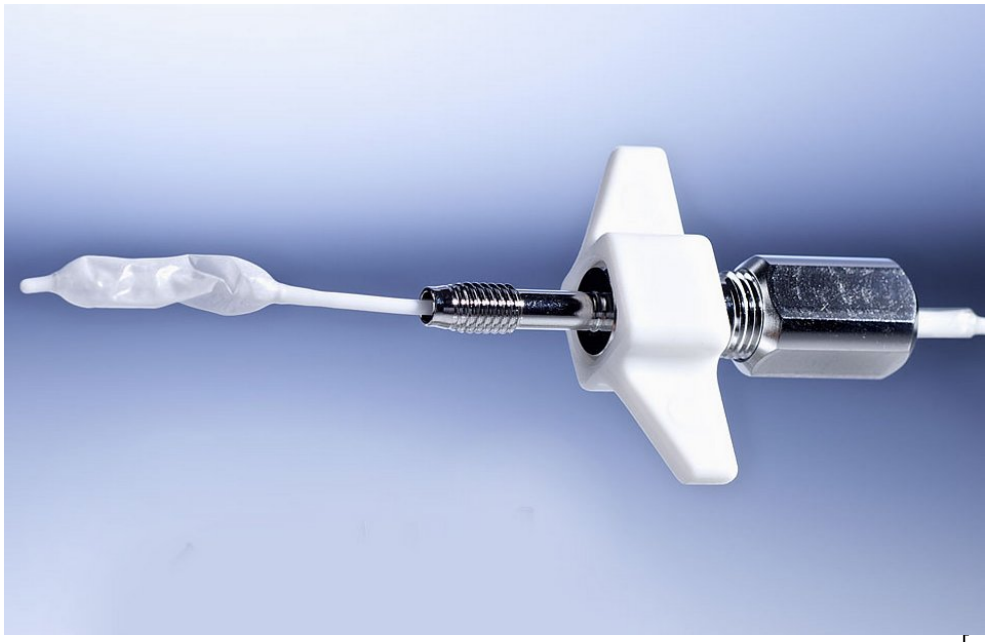

Figure 4. Spiegelberg ICP Sensor,adapted from Spiegelberg website [66]

Of all the micro-transducers discussed here, Neurovent-P, Spiegelberg and Codman are MRI compatible without any danger to the patient, while Camino and Pressio sensors contain ferromagnetic substances that prevent the use of these devices in an MRI environment[43, 44].

Comparing the gold standard ventricular catheterization with micro-transducers, we find that EVD still stands first despite the complication involved as a result of its uses.

The above studies conclude that micro-transducers are as accurate as with ventricular catheterization[22, 40] but possess a common disadvantage or major drawback of re-calibration and drift over time. In summary micro-transducers disadvantages include:

1) requirment of re-calibration in vivo
2) localized pressure measurement without reflecting global pressure
3) no mechanism for CSF drainage to relieve pressure, if high
4) Zero drift over long term measurements

However, the Spiegelberg sensor has ability to self-calibrate every hour, which sets it apart from other micro-transducers. EVD has an edge over micro-transducers due to resetting the transducer to atmospheric pressure and leveling it to the reference/Monro point at any time. Nevertheless, EVD does come with a major drawback of incorrect set up problems beyond the complications due to catheter itself. In EVD, the drip chamber where CSF is drained should be in proximity with the CSF space as CSF drainage depends on the pressure gradient inside the cavity and on the resistance of the drainage, which is set by the relative height of drip chamber. Another major constraint is the three-way valve should be close to drainage to measure the true ICP, if not chances of measuring the drainage pressure is relatively high. This gives rise to false pressure gradients and insufficient CSF drainage that may interfere with the measurement.

Noninvasive ICP Monitoring:

It is incredibly compelling to find an alternative to the traditional invasive procedures, especially when accounting for the associated complications and the expertise of surgeons required. With the noninvasive methods complication such as hemorrhages and infections are greatly reduced creating a demand for improvement in the existing noninvasive ICP technologies. There are several popular techniques used as explained below.

1) Transcranial Doppler Ultrasonography (TCD)

This system uses ultrasound to monitor the changes in ICP. Ultrasound is applied to the middle cerebral artery to monitor blood flow velocity that serves as a predictive factor to estimate ICP. The difference between systolic and diastolic flow velocity is used to estimate the pulsatile index (PI), which seems to correlate with ICP[45,46,47].

$$PI = \frac{systolic\ flow\ velocity - diastolic\ flow\ velocity}{mean\ flow\ velocity}$$

Studies on the correlation between PI and ICP show a correlation factor of 0.439 to 0.938 with a mean deviation of ± 4.2 mmHg compared to invasive measures below 30 mmHg. Deviation seems to increase for higher ICP values and higher correlation boils down to greater individual variation, which is unacceptable for clinical use[2].

On a study by Behrens et al.[48] artificially increased ICP by lumbar infusion, ICP predicted from PI recording were compared with the recording of the Codman sensor. The results showed a 95% confidence interval from -3.8 to 43.8 mmHg for an ICP

of 20 mmHg determined using PI. However, Brandi et al.[49] found that PI calculated through ICP is too uncertain, and the best correlation had a mean difference of -3.2 ±12.6 mmHg. Additionally, this technique demands certain level of training and expertise leading to inter and intra observer variations. Also, this technique has a significant disadvantage, since ultrasound is unable to penetrate in certain patients' skulls which translates to 10-15% disuse[2].

2) Tympanic Membrane Displacement (TMD)

TMD uses the technique of stapedius reflex to estimate the ICP through tympanic membrane movement[50]. CSF and perilymph communicate via a common perilymphatic duct that enables in this estimation. Cochlear fluid pressure has an effect on the movement and positioning. When this system was tested on 148 patients, there was low rate of success that was attributed to increased stiffness of the perilymphatic duct related to aging[51]. Beyond these issues, inter-subject variability was so high in determining ICP through this method it was prohibited fromclinical use.

3) Optic Nerve Sheath Diameter Estimation (ONSD)

Optic nerve shares a part of central nervous system through dural sheath connection. The nerve sheath and white matter have a subarachnoid space in between that changes in diameter in case of ICP elevation. This helps in monitoring using transocular ultrasound. The method has a huge advantage compared to other systems due to minimal time (5 minutes) to estimate ICP, and it is inexpensive. This method has been evaluated and has showed great correlation in estimating ICP, however those studies have excluded

glaucoma and cataract subjects. Research on this technique shows that this method could be good screening test for detecting elevated ICP where invasive ICP monitor or expert neurosurgeons aren't available[52-54].

4) Magnetic Resonance Imaging (MRI) and Computer Tomography (CT)

MRI uses arterial, venous and CSF flow during a cardiac cycle to estimate the CSF velocity and ICP. This method was found to correlate well with invasively measured ICP withR^2 = 0.965 and P<0.005. However, even this method has significant intra-subject variation and hence cannot be used for clinical evaluation[55]. CT on the other hand showed no correlation with ICP in various studies[2].

ICP monitoring methods and principle are diverse as described above; additional methods exists such near infrared cerebral spectroscopy and fundoscopy, all of the methods have significant drawbacks preventing widespread use. Various considerations such as precision, placement of the sensor and complications, etc. must be taken into account when evaluating a method to monitor ICP. Microtransducers accuracy approaches true ICP second to EVD monitoring, if calibration and drifting issues can be resolved. We have established EVD comes with high risk of severe complications. However, it is important to acknowledge the American Brain Trauma Foundation still prefers the EVD for ICP monitoring as their gold standard. Noninvasive techniques have their own shortcoming mainly involving inaccurate measures. For example the accuracy in TCD is 10-15%, TMD is 60% and in ONSD is 10% [2].

Regarding device cost, EVDs are priced about $200, while microtransducers are expensive ranging from $400 to $600 just for the material or sensors[16,22]. Additionally, the cost of maintenance, refilling, surgical procedure to accurately place and position the sensor and the surgeon costs should be considered.

CHAPTER 3

THEORY

Intracranial Pressure - An Overview

Elevation of ICP also known as intracranial hypertension is elevation of the pressure in the cranium. Pressure falling in range of 15-20 mmHg indicates an elevated ICP; 20–25 mmHg being abnormal and aggressive treatment starts at pressures over 25mmHg. Loss of consciousness accompanies pressures exceeding 40 mmHg denoting a high risk state while beyond 50 mmHg, results in brain death. Thus, elevated ICP is a dangerous condition and requires immediate medical attention, monitoring, and treatment[3].

Pathophysiology: Intracranial pressure was first described by a Scottish anatomist Alexander Monro, from whom the Monro-Kellie hypothesis of pressure volume relationship originated. Per Monro's hypothesis;abrain encased in a rigid structure is incompressible, so the volume of the cranial cavity must therefore be constant. The cranial volumes is made up of brain tissue, blood and CSF, and there exists a reciprocal relationship between these, such that increase in one component causes a decrease in the other component(s), i.e. the Monro-Kellie hypothesis[2]. Thus, an increase in any one of the three components will tend to increase the intracranial pressure. Minimal expansion of brain volume does not immediately increase ICP, but once the ICP has reached 25mmHg even small increase in volume can lead to marked elevation in ICP, due to failure in intracranial compliance or autoregulation. In other words, intracranial blood and CSF are the two accommodative components which can compensate for increases in

brain volume. When this compensatory mechanism fails, even small rise in volume leads to large rise in pressure. Brain compliance can be expressed in terms of a compensatory reserve index defined as the ratio of volume change to a pressure change[56].

Cause: Elevation in ICP can be broadly classified by the mechanism that triggers it viz: 1) increase in brain mass due to tumor, edema, hematoma or a medical condition such as liver failure, encephalopathy, etc; 2) elevated blood pressure due to thrombosis, obstruction, or heart failure; 3) changes in CSF production or drainage as in the case of hydrocephalus, meningitis, hemorrhage, or an obstruction in the sagittal sinus. The most common medical conditions include aneurysm, traumatic brain injury, brain tumor, hydrocephalus, stroke and meningitis. However, brain inflammation is observed in the case of chronic implantation of implant/electrodes that arises due to brain tissue-implant interaction[2,3].

Symptoms and Treatments: General symptoms of elevated ICP include headache, vomiting, nausea, altered consciousness, back pain, blurred vision, high blood pressure, behavioral changes etc. Increased ICP is an emergency, and first level of treatment includes monitoring the pressure. Treatment depends on the pressure range and other clinical symptoms associated with the elevation in ICP.

Treatment includes various approaches such as neuromuscular blockade / diuretics / analgesia/barbiturate, osmotherapy (e.g. IV hypertonic solution or mannitol), hyperventilation, improving venous drainage and draining CSF from ventricles of the brain or by a lumbar puncture[56].

Stages of Intracranial hypertension: There are three stages of intracranial hypertension. Stage 1 or primary injury includes minimal and gradual elevation of ICP with all the compensatory mechanics trying to subside the effect. Beyond this point, compensatory mechanisms fails and ICP increases with compromise on neuronal oxygenation and vasoconstriction that leads to increased MAP and CPP, which are characteristic events in stage 2 intracranial hypertension. Stage 3 has continual increase in ICP, for even minimal changes in volume there are dramatic changes in ICP observed. This is due to restricted blood flow to the intracranial space as ICP approaches MAP and these events overall results in increased blood volume in the cranium with elevated ICP and lowered CPP, which becomes an iterative process with positive feedback.

Origin of CSF and ICP - Brain and Ventricle Anatomy

The brain, protected by the meninges has a cushion or buffer fluid around and in between them called the cerebrospinal fluid (CSF). This colorless fluid gives mechanical and immunological protection to the brain 75% of CSF produced by choroid plexus and the rest by the surface of the ventricles and subarachnoid space. CSF is routinely produced and absorbed while it circulates within the cavities in the brain called "ventricles".

Ventricles are a group of cavities having 4 major divisions - two lateral ventricles, 3rd ventricle and 4th ventricle. The choroid plexus is part of lateral ventricle (foramen of Monro), where CSF is produced and circulated through the 3rd and 4th ventricle to the brainstem and subarachnoid spaces covering the brain and spinal cord. There are dural

sinus and subarachnoid granulation that open out to CSF connections over the outer surface of the brain.

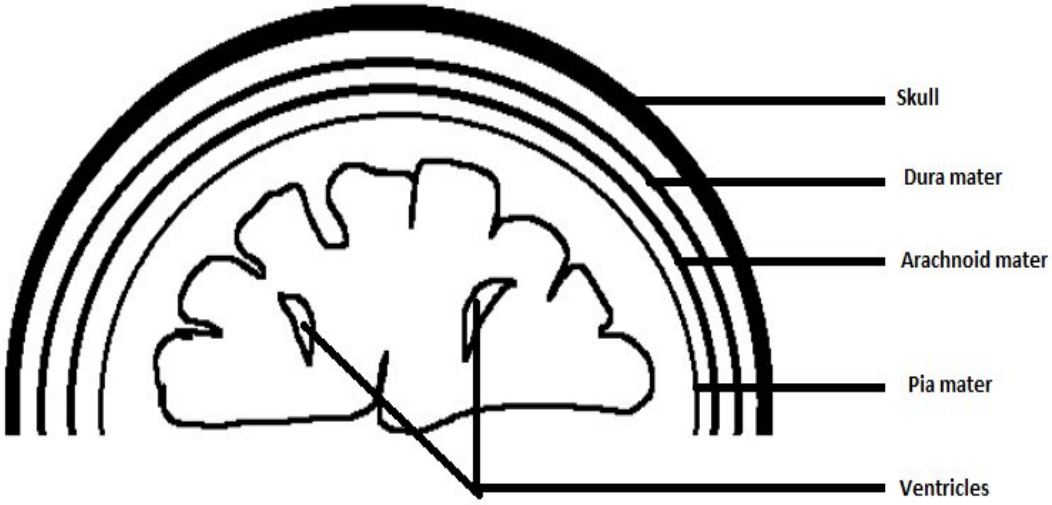

Figure 5. Representation of brain meninges

Correlation with CPP, brain compliance and Equations

ICP is derived from interaction of cerebral blood flow and CSF circulation, which can be represented by this equation:

$$ICP = ICP_{vascular} + ICP_{CSF}$$

The vascular component is difficult to define quantitatively, but CSF component of ICP can be written as:

$$ICP_{CSF} = (Resistance\ of\ CSF\ outflow * CSF\ formation) + Pressure\ in\ sagittal\ sinus$$

Cerebral perfusion pressure (CPP) is an important factor in maintaining the pressure gradient across the cranium, which happens through auto-regulation of cerebral blood flow (CBF). CPP is estimated as the difference of mean arterial blood pressure(MAP) and mean ICP, which could be expressed as:

$$CPP = MAP - ICP$$

When autoregulation fails, ICP has a direct effect on cerebral blood flow. Elevation in ICP causes CPP to decreases, which in turn raises the systemic blood pressure, increasing cerebral blood flow dilating the vessels. This result in increased CBF and ICP further lowers CPP and leads to a vicious circle of events. This causes ischemia, infarction and hemorrhages, fatal to the patient[4, 56].

ICP Monitoring - Waveform analysis

ICP waveforms components

Cerebral compliance can be determined by the ICP waveform, so it is highly essential to monitor ICP continuously with all the events and shifts recorded. A normal ICP waveform follows a sawtooth pattern with three significant peaks - P1, P2 and P3[56].

P1 represents the arterial pressure reflection in ICP transmitted through the choroid plexus, which are consistent sharp peaks. This is termed a percussion wave.

P2 represents the cerebral compliance and is the variable called tidal wave. If P2 exceeds P1 in magnitude, elevated ICP is difficult to manage with medical treatment indicating failure of cerebral compliance.

P3 is the dicrotic wave that reflects the venous pressure and the dicrotic notch from the arterial waveform.

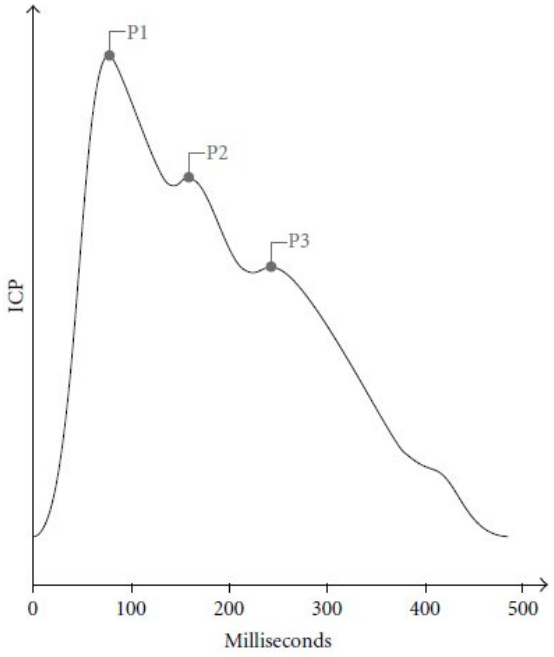

Figure 6. ICP Waveform Components [2]

ICP waveforms types

Lundberg, first classified intracranial pressure variation observed in humans into three distinct types A, B and C waves[4, 56].

A-waves, also known as plateau waves are most significant waves, indicating decreasing cerebral compliance or high intracranial hypertension. These are seen when ICP goes abnormal high 50 to 100 mmHg for 5-20 minutes and then falls abruptly representing neurological dysfunction such as hypoxia, ischemia or infarction.

B-waves are often not significant and are rhythmic oscillations occurring every 1 or 2 minutes associated with respiratory cycle. These represent instantaneous pressure

elevation in 20 to 50 mmHg range. These waves do indicate failure in compliance before the appearance of A waves.

C-waves are a normal ICP waves up to 20 mmHg that follow arterial pressure with frequency of 4 to 8 per minute and signal no pathologically significant failure, i.e. they demonstration everything is normal.

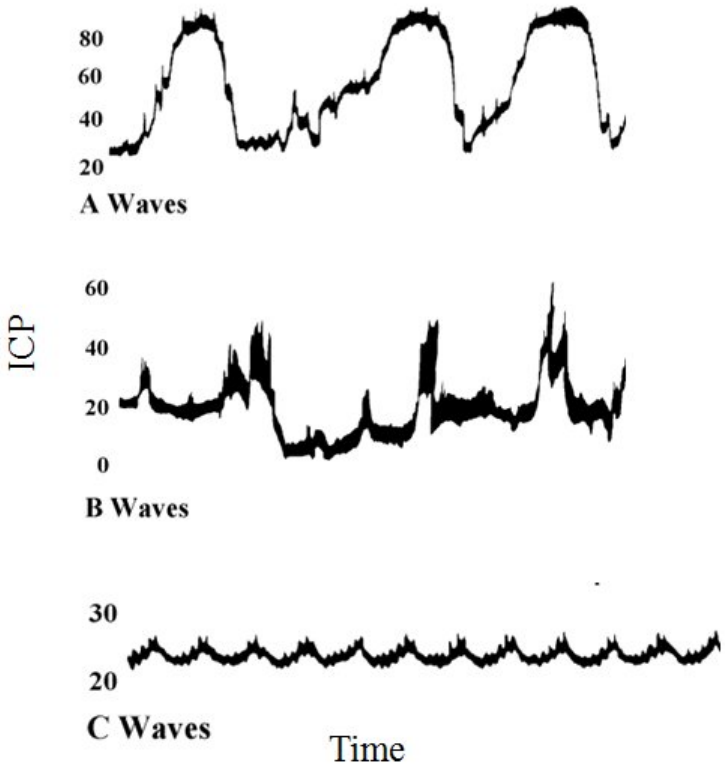

Figure 7. ICP Waveform Types - A, B and C [72]

Spectral Analysis

Analysis of ICP is a whole field of research. ICP analysis, commonly known as high-frequency centroid analysis is based on the power spectrum of a single pulse ICP. The frequency component of ICP ranges from 5 Hz to 15Hz, with dominant fundamental

peaks representing slow and respiratory cycle waves. A standard power spectrum of ICP is as shown below.

The waves - slow, respiratory and pulsatile ICP waves overlap in the time domain and hence, cannot be visualized. In the frequency domain representation, they are clearly separated. The literatures describes the use of the power spectrum analysis of slow waves form as a predictor for intracranial hypertension and low magnitudes in the slow waves are associated with failure of autoregulation, resulting in fatal events[57].

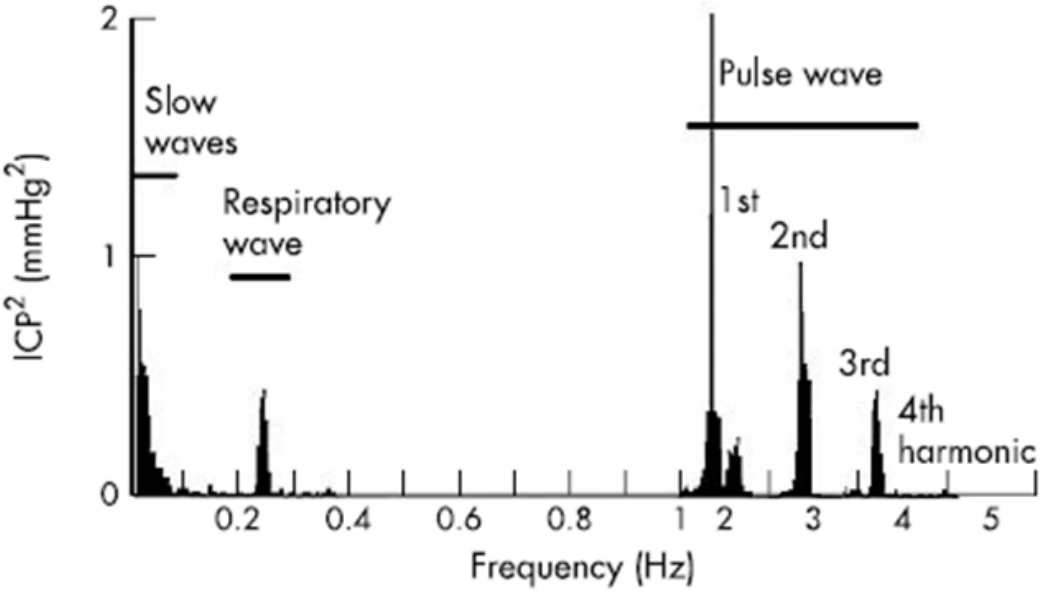

Figure 8. ICP Spectrum [4]

Sensors

Force Sensitive Resistors

Force sensing resistors (FSR) are conductive polymers, whose resistance changes are indicative of the force or pressure applied on the surface[58, 59]. The FSR technology was invented by Franklin Eventoff and patented in 1977. Interlink electronics was founded by Eventoff in 1987 based on this technology and later Sensitronics became the

leader in this technology, which is his company founded in 2001. FSRs are commercially available as sensors or sheets that can be customized for the application of interest. These are also available as pressure sensitive inks in certain countries to screen print on the substrate. The pressure sensitive ink consists of both conductive and non-conductive particles in a matrix suspension. The choice of conductive material, non-conductive material and the suspension depends upon the application and the manufacturer.

Principle:

The sensor used in this work operate on the principle of piezoresistivity, which is change in resistance due to a change in mechanical force applied over the sensing area. This change in resistance can be measured as a change in voltage to quantify it. Advantages of using FSRs is that they can tolerate hostile environments, are low cost, and have good shock resistance. They were also chosen for their low profile compatible with human physiology for epidural or subdural monitoring, the thickness is usually less than0.5mm.

Construction:

The sensor has two pressure sensitive layers on a flexible PET substrate with a screen printed conductive pad extending from sensing area to connection port. The sensing layer is an ink having both conductive and non-conductive microparticlesin a matrix. Sandwiched between the layers on the periphery is a very thin material called “spacer”, whose thickness determines the minimum force required to activate the sensing property[60]. There are two types of FSR based on construction: ThruMode and ShuntMode

1) ShuntMode: In this type of FSR construction the resistive ink material is printed on one film and the interdigitated pattern of conductor on the other, then both are put together facing each other with a spacer in between or on the periphery.

2) ThruMode: This is another type of FSR construction, where both the films have resistive ink material printed over a solid conductor printed on the substrate.

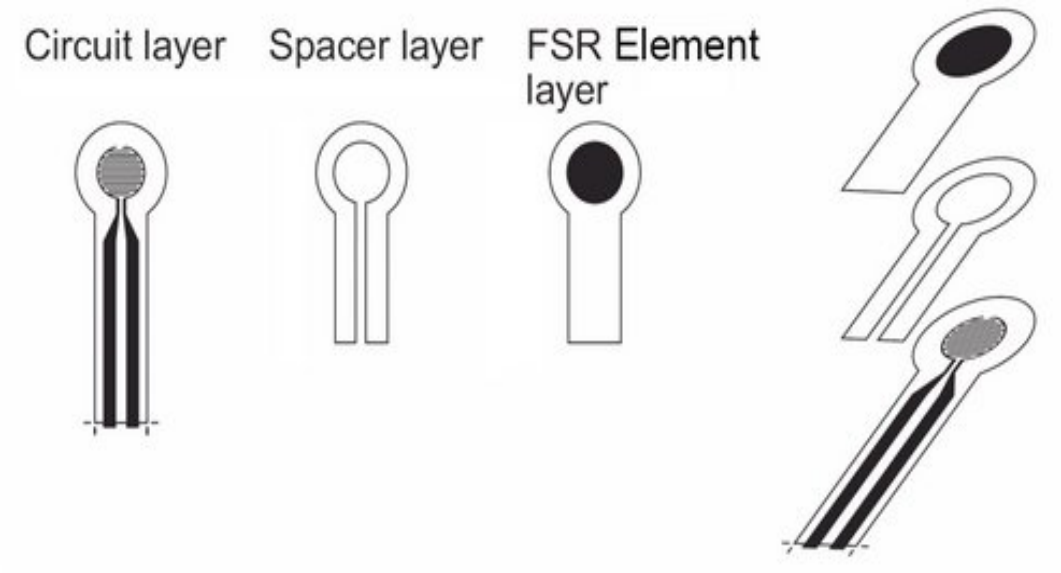

Figure 9. Construction of ShutMode FSR [67]

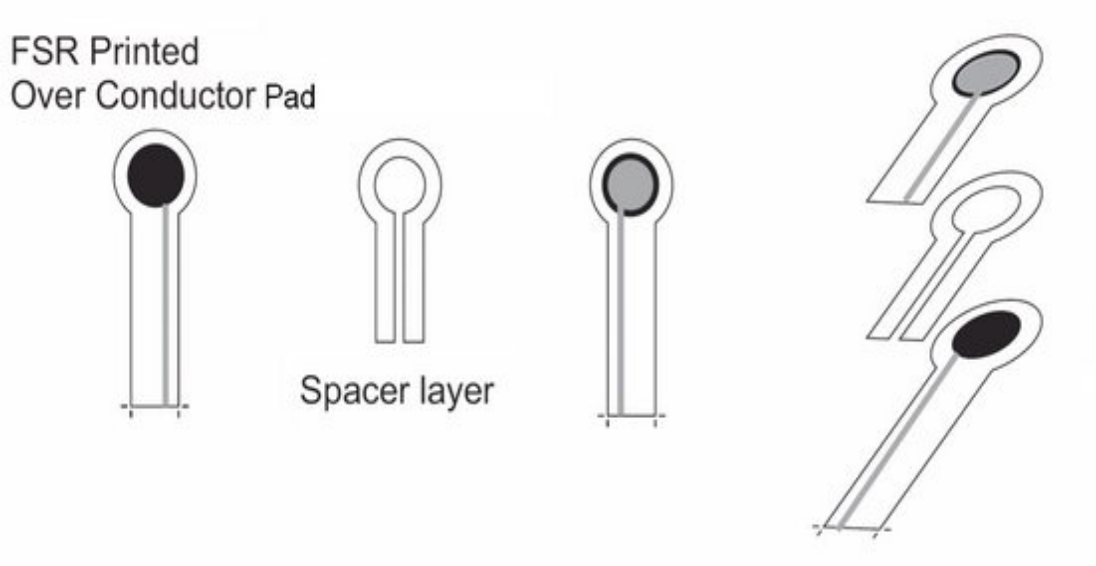

Figure 10. Construction of ThruMode FSR [67]

In general, ThruMode FSRs are more sensitive than the ShutMode FSRs. FlexiForce and Sensitronics FSR were investigated for low pressure application. *Sensitronics'* Force Resistive Sensors were more sensitive for our application and were chosen for investigation.

MicroElectroMechanical Systems (MEMS) Sensors

MEMS technology is fast growing, and its biomedical applications has been vast. Owing to their micro-scale structures and features, and ease of integration with siliconelectronics, MEMS are poised to maintain enormous growth in biomedical devices. Within these MEMS devices for biomedical applications there is a large research focus on piezoresistive technology. We have selected one such device for this work. *Measurement Specialties* disposable blood pressure transducer was chosen in our investigation of sensors for brain pressure monitoring. Model No:1620 with MEMS die

is batch manufactured and available in a 10x12 element array with antistatic protection for commercial use[68].

Construction:

This is a fully piezoresistive silicon pressure transducer is used for invasive blood pressure monitoring and calibrated per the Association for the Advancement of Medical Instrumentation (AAMI) standards. This sensor has a MEMS die of 2x2 mm square, mounted on a ceramic substrate with a plastic encasement and a cup extension over the sensing area, where the die is exposed for sensing purposes. A silicone dielectric gel over the die in the cup provides electrical and fluid isolation.

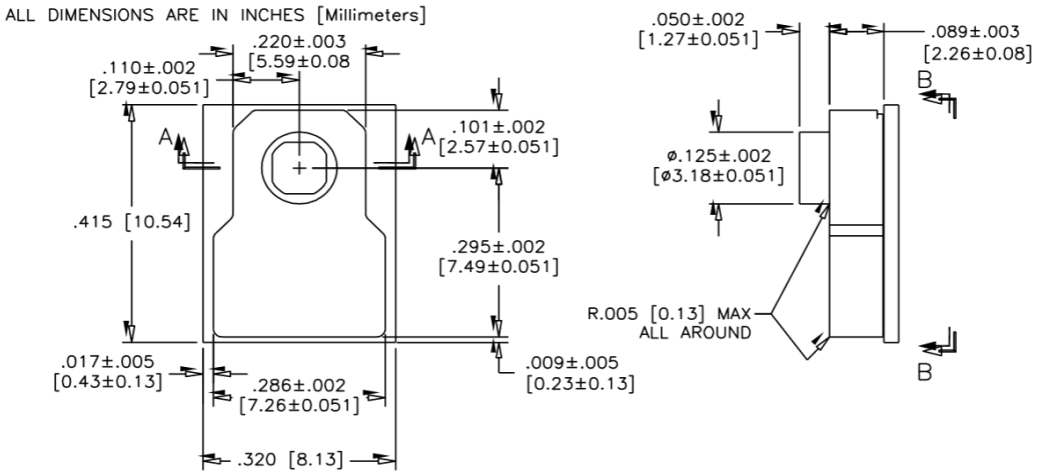

Figure 11. Dimensions of the MEMS Sensor [68]

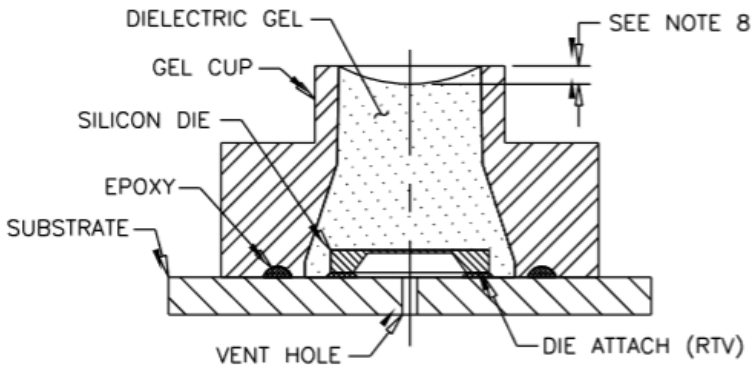

Figure 12. Construction of the MEMS Sensor [68]

Features and Application:

This miniature transducer is low-cost and designed for medical application complying RoHS regulation. This device is designed for invasive blood pressure and intrauterine pressure monitoring. The sensitivity is typically 5uV/V/mmHg with range of measurement -50 to 300 mmHg and frequency response 1200 Hz. This is an active transducer and requires a voltage supply to function. The operating lifetime is 168 hours or 7 days with shelf life of 5 years.

Principle and Working:

The sensor works like a strain gauge with the MEMS die within. The changes in pressure are reflected as changes in resistance that can be quantified. From resistance formula,

$$Resistance = \frac{Resistivity * Length}{Area\ of\ the\ conductor}$$

so for changes in material dimensions (length or area) the resistance either increases or decreases indicative of the strain/pressure applied over it. This transducer has four such resistances allowing a Wheatstone bridge configuration, where two transducers increase

in resistance while other two decreases with incident pressure.This configuration increases the gain of the system, increasing accuracy.

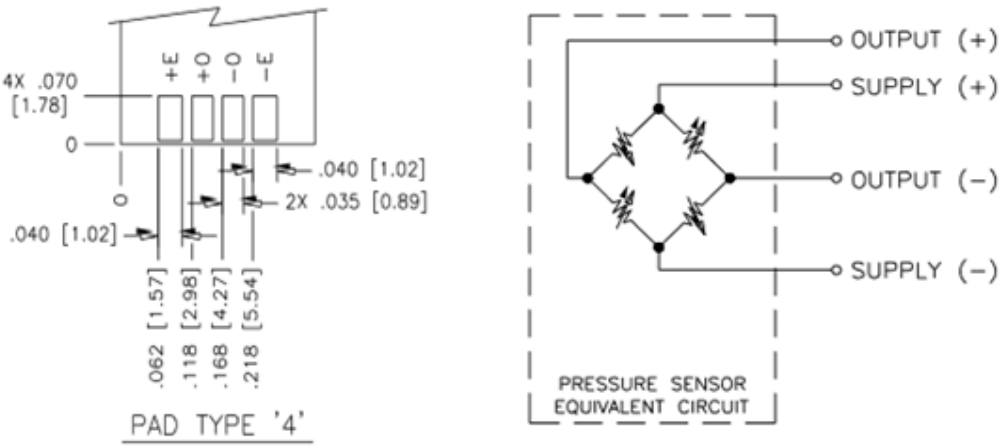

Figure 13. Sensor pins internal connection - equivalent circuit [68]

CHAPTER 4

METHODOLOGY

Research Trajectory

My research, which started with investigation a very specific problem, later turned out to be a great solution for general low-cost brain pressure monitoring. Thus, the system was tested in such a manner that we could conclude on its performance generally, rather than solely as an augmentation of an ECoG array.

Initial investigation: Force sensing resistors (FSR) were initially investigated as a pressure sensitive device for measuring the pressure in the range of 0-100 mmHg. Commercial FSRs are used for higher pressure ranges (0.5 - 50 psi), thus generally measures beyond 25.86 mmHg pressure. For the purpose of evaluating low pressure changes, modification in the sensing area was necessary. Sandwiched between the two layers of the pressure sensitive layer, is a spacer material, the thickness determines the minimum force required to activate the sensor. This technical aspect was explored while interacting with the inventor of this technology Mr. Franklin Eventoff. I utilized this concept for my study and the spacer material was changed for low pressure application. This is a novel approach and in the intensive literature review that I performed, there is no record of this concept or of the sensor being utilized for an ICP monitoring application. I studied *Sensitronics'* FSR without and with a thinner spacer material. The results were not highly satisfactory due to the non-uniform dispersion of ink and part to part variability that was magnified in the low pressure range. So, further experimentation on these sensors were suspended.

Further investigation: Having the main focus on piezoresistive technologies for intracranial pressure sensor, *Measurement Specialties'* disposable blood pressure sensor was considered next for testing. The fact that this sensor has been on the market and has been utilized by various companies to manufacture extravascular blood pressure transducer catheters (which are approved by FDA) showed the efficacy of this sensor. Further, the dynamic range of this transducer is broad enough to measure ICP changes and follows the AAMI specification for ICP monitoring. Additionally, literature study indicated no substantial use of this transducer for epidural intracranial pressure monitoring. These findings were encouraging with respect to the use of the sensor for ICP monitoring, and we believe this is a great solution to ICP monitoring. Therefore, to secure a proof of concept an epidural ICP monitoring system was developed, with an aim to integrate it with the ECoG electrodes in future. This was achieved by modifying the sensing area. A sensing cup attachment was made at the site of sensor's original sensing area. Sensing cup was glued with super glue to the sensor. The experiments described below were performed and evaluated with this sensing cup extension.

Design and Working

FSR

(i) Sensor Modification: Spacer material is typically an adhesive membrane that acts as a double-sided tape. These membranes are commercially manufactured by 3M. *Sensitronics'* one inch ThruMode FSRs were used for my research, which had a 0.13mm thick spacer material. This 0.13 mm thick spacer (3M 7945MP) was replaced by a 0.09 mm thick spacer (3M 7953MP) material for the low pressure application to reduce the

threshold pressure of actuation. This construction, property defines the operating range of these sensors[67].

Product	Adhesive 1 Thickness mils (mm)	Carrier Type Carrier Thickness mils (mm)	Adhesive 2 Thickness mils (mm)	Liner 1 Type Liner Thickness mils (mm)	Liner 2 Type Liner Thickness mils (mm)
7953MP	1.5 mils (0.04 mm)	Polyester Film (PET) 0.5 mils (0.01 mm)	1.5 mils (0.04 mm)	58# Polycoated Kraft Paper (PCK) 4.2 mils (0.11 mm)	58# Polycoated Kraft Paper (PCK) 4.2 mils (0.11 mm)
7945MP	2.0 mils (0.05 mm)	Polyester Film (PET) 1.0 mils (0.03 mm)	2.0 mils (0.05 mm)	58# Polycoated Kraft Paper (PCK) 4.2 mils (0.11 mm)	58# Polycoated Kraft Paper (PCK) 4.2 mils (0.11 mm)

Figure 14. Spacer construction with material specification[69]

(ii) Circuit Design for Implementation: Resistance changes in the sensor are indicative of the pressure variations over the sensor and measurement of this dynamic variation requires a circuit. This readout circuit could be a voltage divider or bridge circuit. For simplicity a voltage divider was chosen; it consists of a 2 V supply voltage, a fixed resistance of 100 Kohms in series with the FSR, which acts as a variable resistor depending on the applied pressure. The output voltage increases as the resistance of FSR decreases. This relationship can be quantified by the equation below from Ohm's law:

$$Vout = \frac{Vin * R}{(R + FSR)}$$

The output from the circuit board was directly connected to the computer through a data acquisition (DAQ) system hardware (Measurement Computing USB 1408FS) interfaced with a real-time acquisition program in MATLAB written as a part of this research, specifically created for this application.

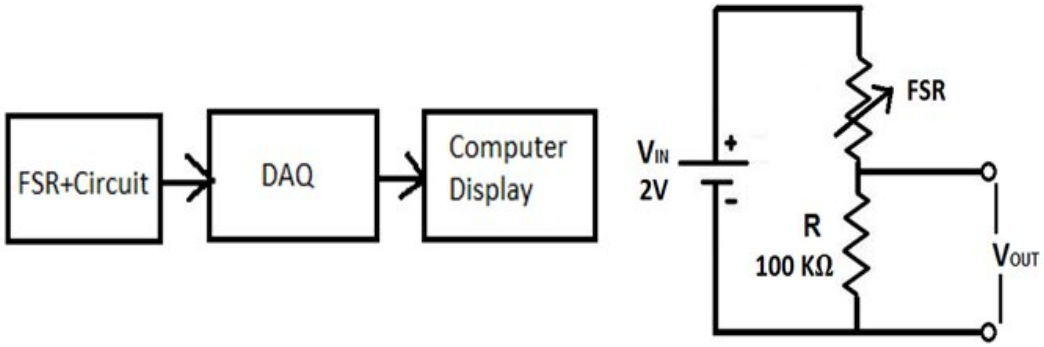

Figure 15. Block diagram and circuit diagram of FSR based pressure system

Figure 16 showing the sensor's behavior during loading/application of force demonstrating the relationship between the resistance and pressure. With no load or application of any pressure over the sensor, the resistance is very high on the order of several thousand kohms and on loading decreases according to the pressure applied.

Note: The plot isn't a calibration graph as the parameters and construction is modified in this work.

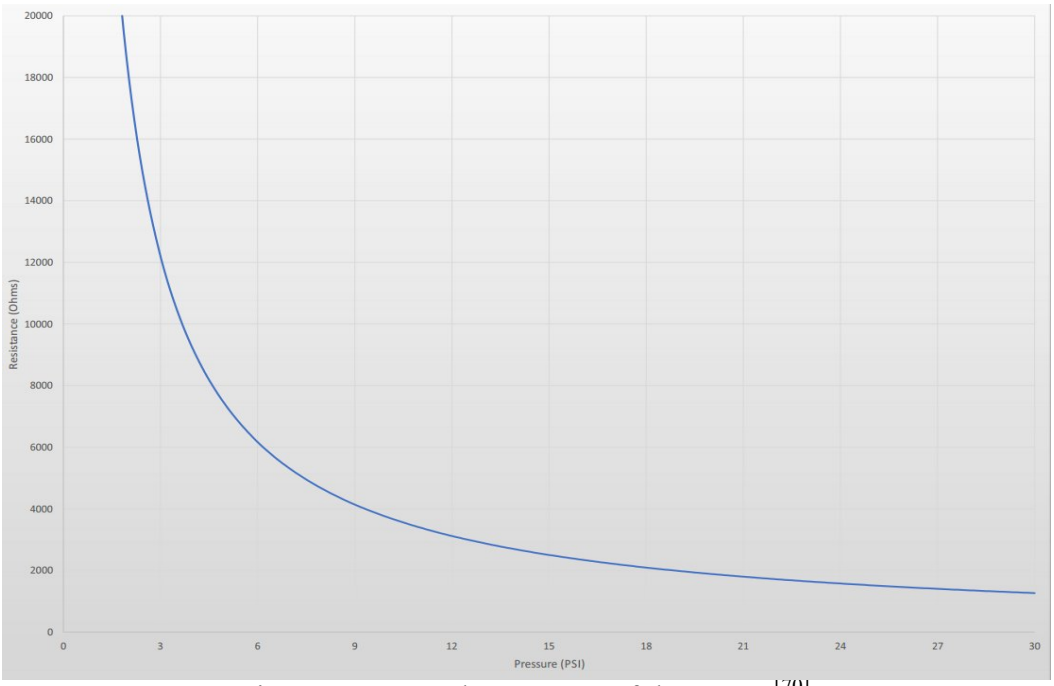

Figure16. Example response of the sensor[70]

MEMS Sensor

(i) Sensor Modification: The sensing area requires a physical modification to provide access into the epidural space. The sensing cup extension or packaging is specific for the implementation model considered. However the geometry of this model used is capable of enabling implementation on another model. Here it is executed for an epidural application in rats.

A sensing cup (as show in the figure below) is a conical tapering polypropylene pipette tip cut down under a microscope to exactly fit the outer diameter of the sensing area projection on the sensor. This cup is designed for a rat craniotomy having 2 mm drill size, where an opening of 1.7 mm is exposed inside the rat skull, which is <1 mm deep (the skull thickness) from the access point of2 mm diameter of the cup that fits on the skull as shown in the figure 17. The sensor is attached at the end with the larger opening

as seen in figure 18 and the sensing pocket/cup is filled with saline as the incompressible pressure transmitting medium before the implantation or testing.

Note: The sensing cup directly fits onto the head and is sealed directly onto to the skull with no bolt requirement.

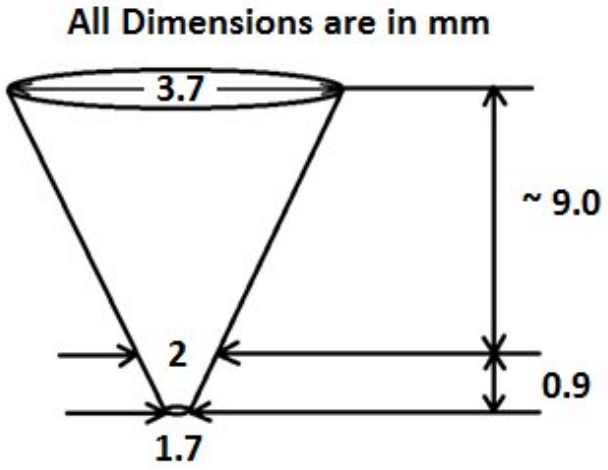

Figure 17. Sensing cup dimension

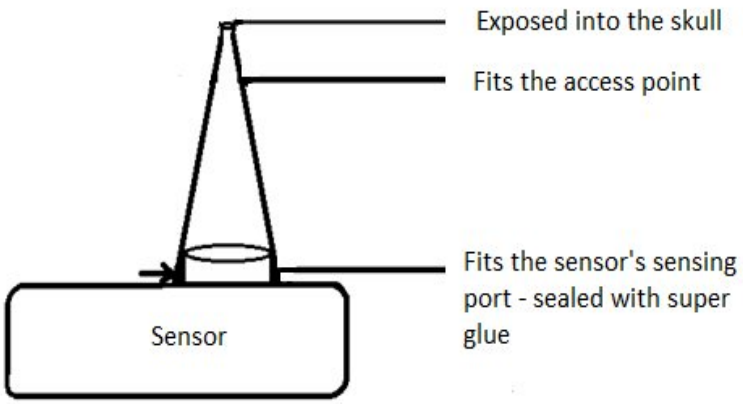

Figure 18. Sensor modified with sensing cup attachment

(ii) Circuit Designed for Amplification and Processing: The sensitivity of the transducer is 5uV/V/mmHg, representing the need for voltage amplification to accurately measure pressure changes. The transducer needs a voltage supply, which here is fixed at 6V making the calibration factor 0.030mV/mmHg for reconverting the voltage to pressure values. The circuit designed has two main parts, a voltage regulator that provides a 6V supply to the sensor from a 9V battery and an amplifier with a 1000X (or) 60db gain. To avoid noise, the whole circuit runs on battery power, which also makes the system very portable.

The voltage regulator circuit uses LM317 IC, capacitors, and resistors, to provide a 6V output from a 9V battery. This supply goes to the positive voltage pin of the sensor, the positive and negative voltage outputs of the sensor are given to the respective pins of the amplifier chip. The negative pin of the sensor is grounded with respect to the 6V DC supply for the sensor.

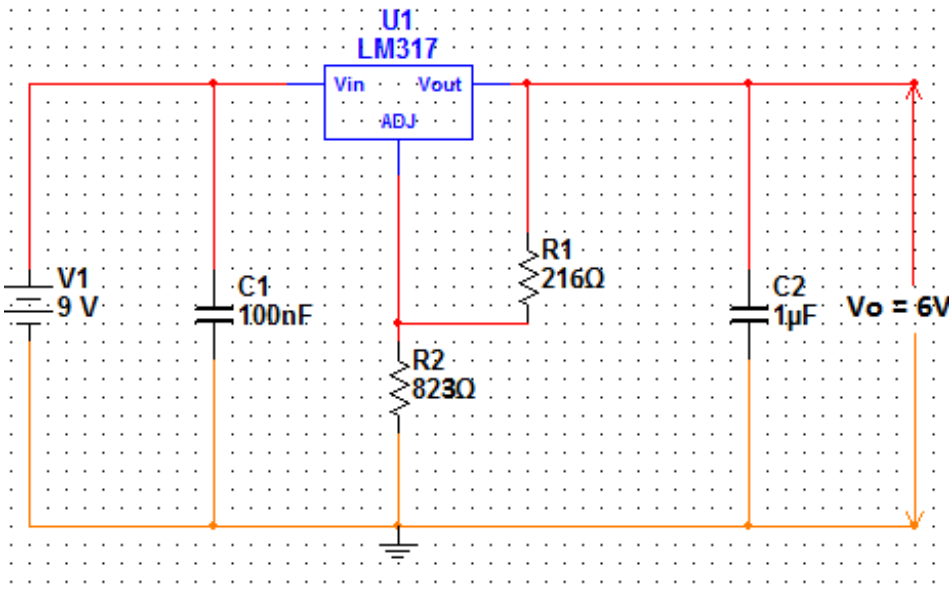

Figure 19. Voltage regulator circuit

The amplifier circuit consists of an instrumentation amplifier INA101, resistors, power supplies and potentiometer. The gain is set with a single resistance across pin 5 and pin 10, which is calculated from the equation below:

$$Gain = 1 + \frac{40K\Omega}{Rg}$$

where, Rg is the resistance fixed to obtain the desired gain. Here, Rg is set as 40Ω to have a gain of 1000 to convert the mV to V. The IC requires a supply of min ±5V and in the design ±9V is provided at pin 2 and 13 respectively. The output from pin 1 and 14 runs to the DAQ that is interfaced with a real-time acquisition program in MATLAB specifically created for this application. Pin 14 is grounded and common ground exists between amplifier and voltage regulator circuit to avoid any noise in the output. Pins 6 and 7 are given to a 100kΩ null potentiometer to provide an offset adjustment by the user, which can control the baseline offset that pressure transducer may have. Also, the center pin of the potentiometer is connected to a positive supply. Below is a figure showing the pin diagram of the INA 101 instrumentation amplifier and the circuit connections.

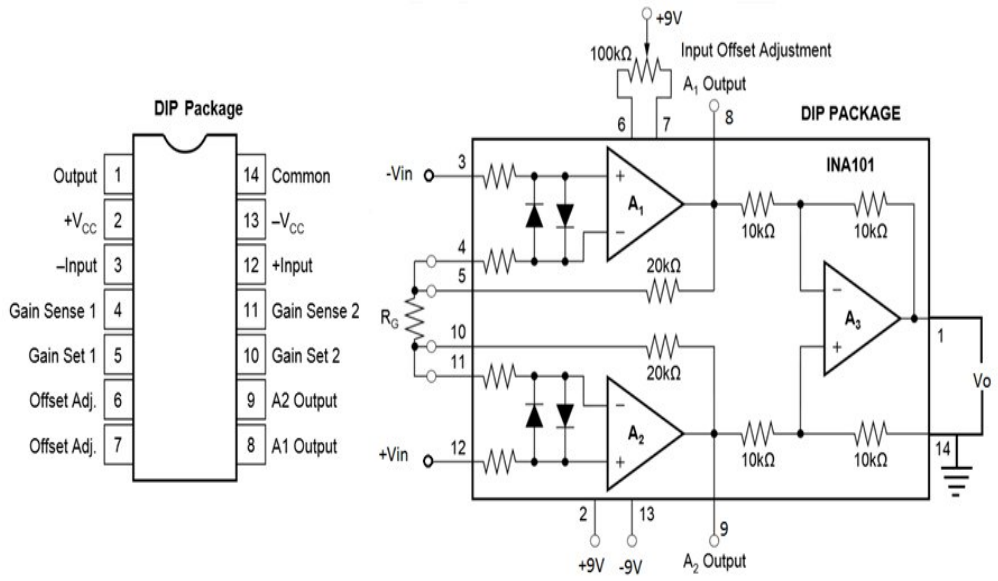

Figure20. Pin connections and amplifier circuit[71]

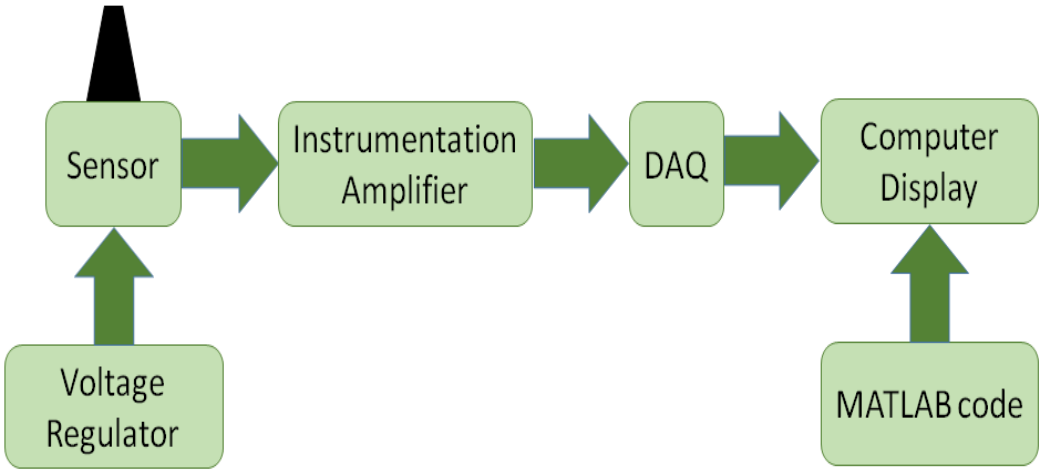

Figure 21. Block diagram of the sensor and electronics

Experimental Procedure

Bench Tests

Calibrationof the FSR:

Calibrated Weight Test: Calibrated weights from 1g to 350g were placed on the sensing layer with an acrylic disc to uniformly distribute the pressure over the area. Weights were added in increments of 1g from 1g up to 20g, and then in increments of 5g from 20 g to 50 g, and 10g from 50-350g; this procedure is considered one experiment With the readings observed, a calibration graph was plotted for equivalent pressure for these weights versus the output voltage. Three sets of calibration experiments were performed to determine the calibration parameter used in the signal reconversion program. The setup is developed based on previous studies for the same sensor[61, 62].

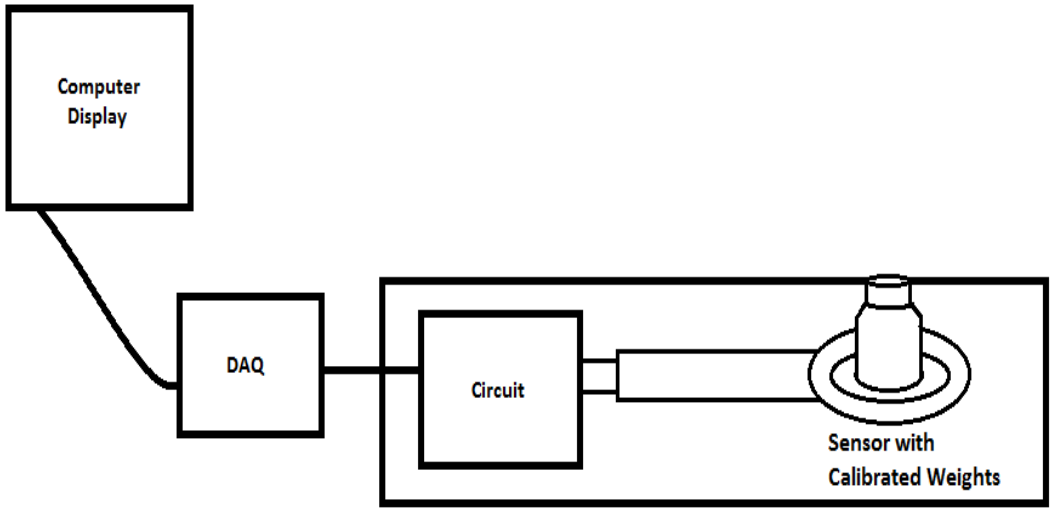

Figure 22. Calibration Test Setup with Weights

Measurements with the FSR:

Water Column Test:

A 90 cm long acrylic column with the sensor's sensing layer taped down onto an acrylic plate was constructed for this test. The set up was sealed at the junction of the column and the acrylic plate on which the sensor was taped down. Epoxy putty was used for sealing around the perimeter to prevent any leaks. The other end of the column was partially closed during experimentation with openings only for the tubes to purge in water for evaluation. Water was purged manually in steps of 1 cm to a height of 60 cm and equivalent pressure values were calculated. Three initial experiments were performed to determine if the calibration range in signal reconversion program matches the measurement obtained in these trials. Discrepancies usually occurred due to slight tilt in the water column. This happens due to the pressure water exerts on the side walls as water is added in. This error was corrected by manually leveling the system with a bull's eye leveler. Once error-free and calibrated, three sets of measurement experiments were performed. The setup was developed based on previous studies with the sensor[63].

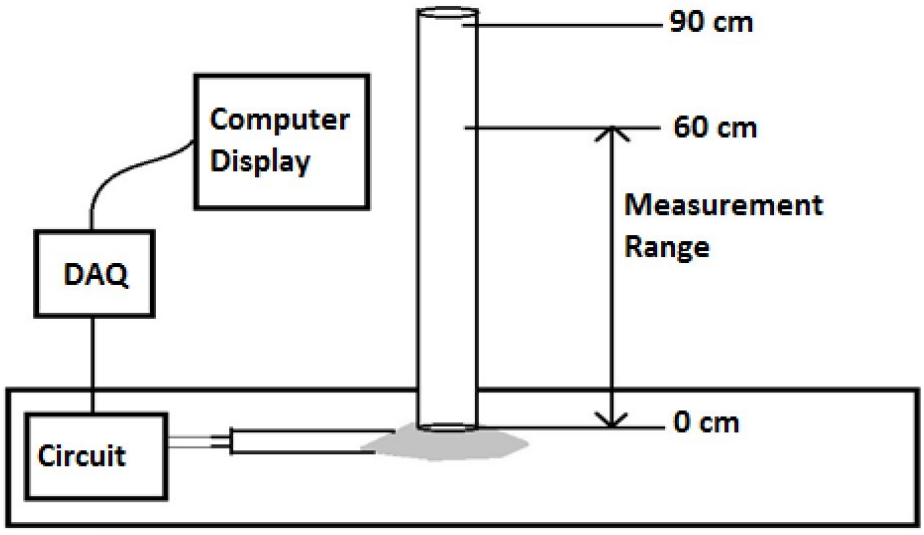

Figure 23. Water column measurement setup

MEMS Sensor Calibration:

1) Sensor Calibration: The first time the sensor is removed from the manufacturer's packaging, the sensor is calibrated as per the manufacturer's recommended calibration technique. A 150kΩ resistor is connected between the positive voltage output pin and the supply input pin of the sensor, which must provide equivalent voltage for 100 mmHg, which is 0.030mV for a 6V supply. But, in practice 0.029mV was observed for a 5.89V supply voltage.

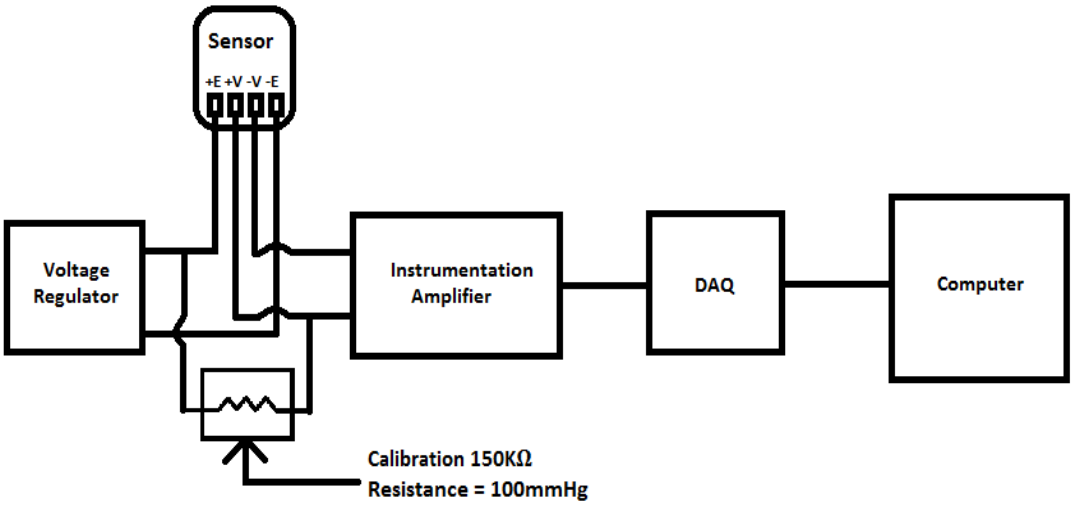

Figure 24. Calibration of the sensor

2) System calibration: This calibration was performed to determine if the calibration factor set in the voltage to pressure reconversion program is accurate. Sensitivity according to the manufacturer is typically 5uV/V/mmHg, and ranges between 4.95 uV/V/mmHg to 5.05uV/V/mmHg. The calibration factor, in the reconversion program is set based on this sensitivity multiplied by the supply voltage. For a 6V supply, calibration

factor is 0.030mV/mmHg, but in practice it is set as 0.02945mV/mmHg for an observed sensor supply voltage of 5.89V.

A centrifuge tube was used to provide a static water level at a particular height, used to calculate the pressure exerted by the column of water over the sensor. This true calculated pressure was compared to the pressure measured by the sensor. Any errors or baseline shifts obtained at this stage are adjusted to obtain an error free reading. Below is the figure illustrating the setup described, in which the opening of the centrifuge tube is customized to exactly fit onto the sensing cup. The distance from the opening of the centrifuge tube to the opening of sensing cup is measured as 11 cm and the height of the sensing cup is 1 cm. Thus, the setup can measure a maximum of 12 cm water height or 8.8mmHg. Three values of static pressure (2mmHg, 4mmHg and 8mmHg) were measured to check our measurement against calibration or actual pressure.

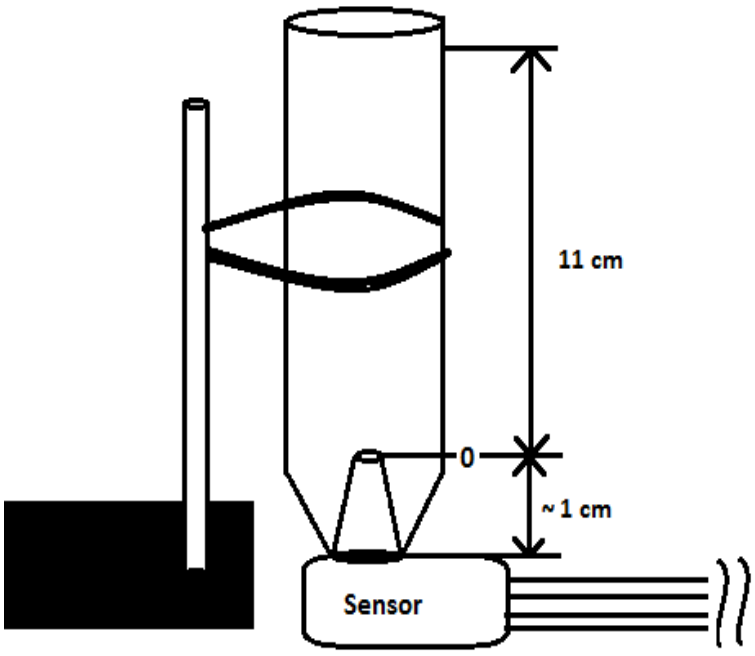

Figure 25. Experimental setup of water column for system calibration

MEMS Sensor Measurement:

1) Static Pressure Test: This test was accomplished using the centrifuge tube with water to measure pressures from 0 mmHg to 8mmHg. The above mentioned water column setup was utilized for this experiment and three experiments were performed with pressure steps of 0.5mm Hg.

2) Dynamic Pressure Test: This test was performed to qualitatively evaluate the response time of the system. Since, there was no delay element added in the system, it was assumed to work per manufacturer's determined frequency response of 1200Hz, implying that the response time is approximately 1ms. This setup consists of a sphygmomanometer with a centrifuge tube attachment instead of a standard blood pressure cuff. The centrifuge tube is customized to provide access to the sensor via the sensing cup. The medium used for this test is air. The experiment is performed by pumping and releasing the air, though the bulb of the sphygmomanometer. Each set of experiment consists of a pump and release cycles equally timed every second for one minute. Three sets of experiments were performed

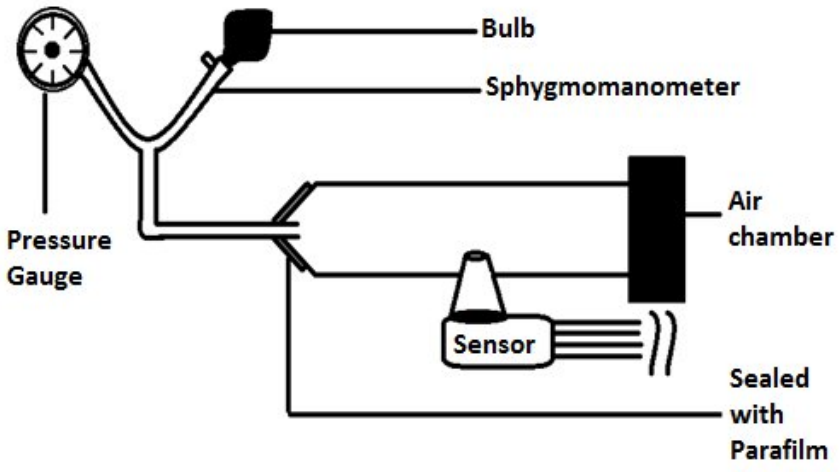

Figure 26. Dynamic Pressure Evaluation Setup

3) Media Test: The static water level setup was used for this experiment with saline to determine the effects of an electrically conductive media on the system, if any. Phosphate Buffer Saline (PBS) 10X and 1X were used to test with a medium having nearly equivalent characteristics of physiological saline. Pressure measurements from 0-8 mmHg with steps of 0.5 mmHg were performed, and three sets of such experiments were repeated.

Animal Model Test

Surgical setup and procedure:

The animal model used for this study was rattus norvegicus. The animal was anesthetized with a ketamine/xylazine/acepromazine cocktail, and then the animal was placed on 1-3% isoflurane gas through a nose cone mask. The animal's head was shaved, and the surgical site was prepared with a betadine scrub followed by isopropyl alcohol rinse, repeated 3 times. The animal was then mounted onto a small animal stereotaxic mounting apparatus on a heating pad and covered with a sterile drape, and eye lubrication was be applied. A tail catheter was placed to deliver hypotonic saline and mannitol. An incision was made with a sterile #10 blade along the midline extending from just behind the eyes to the base of the neck. The scalp was retracted and the bone was cleaned of the periosteum. A 2 mm diameter craniotomy was performed using a surgical drill.

Once the sensor is in its desired position, cyanoacrylate was used to secure the sensor to the skull. The intracranial pressure was recorded and manipulated as described below. The animal was euthanized following the experiment.

Experimental procedure:

Table 1

Tabulation of experiment procedure followed in animal model testing

Indication/Expected Response	**Drug/Manipulations**	**Infusion/procedure time**	**Data collection time**
Baseline ICP	None	None	4minutes
ICP Variations	Mechanical Compression	2 minutes with compressions every 10seconds	2 minutes repeated 3 times
Increase in ICP	Hypotonic Saline	3 minutes	5 minutes
Decrease in ICP	Mannitol	8 minutes	2 hours

After the craniotomy, the sensing cup was filled with saline and any offset due to this cup hold saline (~ 0.8mmHg) was reset to zero. A final check of the sensor with the sensing cup was performed for calibration and error using the sphygmomanometer to measure 0-20 mmHg; this is done just prior to introducing the sensing cup into the skull. The sensor and the sensing cup filled with saline were turned upside down and placed into the rat's head reaching its dura. Since, the sensing cup is customized for a 2mm burr hole to fit the skull with 1.7mm diameter opening for pressure contact, given the skull thickness is about 1 mm. The wire connections from the sensor were taped down over the sterile drapes covering the rat's body for stability, preventing jolting of the sensor. Once, the baseline pressure value correlating to the heart rate was observed, confirming the

sensor was working properly, the sensing cup was sealed onto the skull with cyanoacrylic glue.

The mechanical compression procedure involved timed compressions of the rat's abdomen or thorax every 10 seconds for 2 minutes. This procedure was adapted from various literatures demonstrating the ability to change ICP in accordance with compression (increases ICP) and relaxation (returns to baseline ICP).

Hypotonic saline was injected to bring about an increase in ICP. A 40 ml/Kg 0.45% hypotonic saline was introduced through the tail catheter while ICP was recorded.The expected response time for hypotonic saline is under 2 minutes. Thus we observed the ICP for 5 minutes following the initiation of the bolus.

Mannitol was injected to bring about a decrease in ICP. Mannitol was injected after 5minutes from the end of hypotonic saline injection. This was injected over 8 - 9 min interval and ICP was expected to start falling 20 minutes from end of mannitol injection. See Appendix 1 for a photograph of the implanted sensing cup.

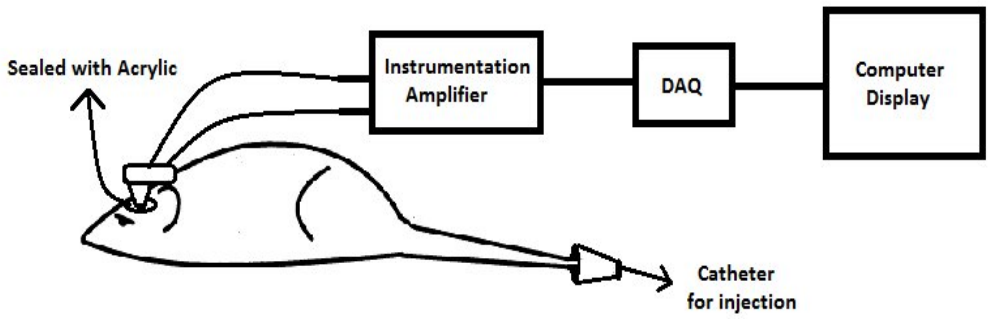

Figure 27. Animal model Experimental Setup

CHAPTER 5

OBSERVATION AND INFERENCE

Bench Test FSR

Calibration

The force sensing resistor was modified to decrease the range of sensitivities to match the ICP range by replacing the spacer material with a thinner spacer. After spacer modification, the FSR was calibrated with known weights. This procedure involved calculation of pressure from the weights,given the area of the sensor. Calculations, are as follows:

We know that,

$$Area = \pi r^2$$

$$diameter\ (d) = 1inch = 25.4\ mm$$

$$radius\ (r) = \frac{d}{2} = \frac{25.4}{2} mm = 12.7\ mm$$

Therefore,

$$Area = 3.14 \times (12.7)^2 = 506.45\ mm^2 = 0.506 \times 10^{-3} m^2$$

$$Pressure\ (P) = \frac{Force}{Area} = \frac{mass \times acceleration}{Area}$$

Where,

$$acceleration = 9.8\ m/s^2$$

$$mass\ varries\ between\ 1\ g - 350\ g$$

$$P = \frac{mass \times 9.8}{0.506 \times 10^{-3}}\ N/m^2$$

This estimates the pressure over the sensor and serves as calculated pressure. The voltage during each weight increment is noted and plotted on the calibration curve.

The increments were 1g from 0-20g and 5g from 20-50g and 10g from 50-350g.

A voltage versus estimated pressure is plotted and a nearest polynomial fit was used to determine the calibration equation for pressure reconversion during measurements. The data observation followed a fifth order polynomial equation as follows:

$$P = 33V^5 + 14V^4 - 90V^3 + 51V^2 + 14V + 19$$

The figure below shows the nearest polynomial fit for the observed voltages and the respective pressures. This polynomial fit equation is used to estimate the pressure over the sensor when a voltage is measured to determine the piezoresistive change brought about by a change in pressure.

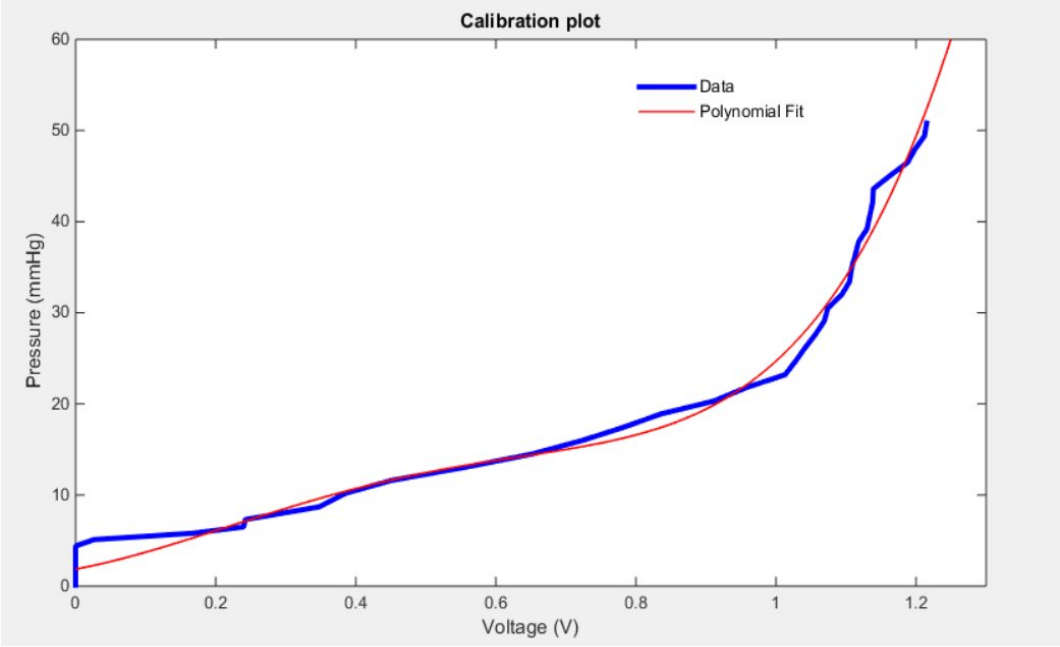

Figure 28. Calibration plot of FSR.

This plot represents the voltages observed for the respective applied pressure; The data was fit with a polynomial curve of fifth order. This equation is used to determine the intracranial pressure during measurements.

Measurement

Three sets of experiment were performed to measure 0 - 50 mmHg in increments of 0.7 mmHg or 1cm height of water level. And the pressure observed in the three sets of experiment averaged.

Pressure due to water increments in the column is calculated to find the estimated pressure as below.

$$P = \rho h g$$

Where, P = pressure (pascal); ρ= density of water, which is 999.9 kg/m^3; h=height of water in the column (m); g=acceleration due to gravity, which is 9.8m/s^2

$$P = 999.9 \times h \times 10^{-2} \times 9.8$$

$$= (97.99 \times h)\ Pa$$

$$=> P = \frac{97.99h}{133.32}\ mmHg = (0.7h)\ mmHg$$

The converted/measuredpressure is plotted with the calculated pressure to find the deviation in the readings. It's important to note that the measured pressure is based on the polynomial calibration equation. Below is a figure of measured voltage against the calibration curve representing the overall qualitative repeatability in the measurement of the sensor.

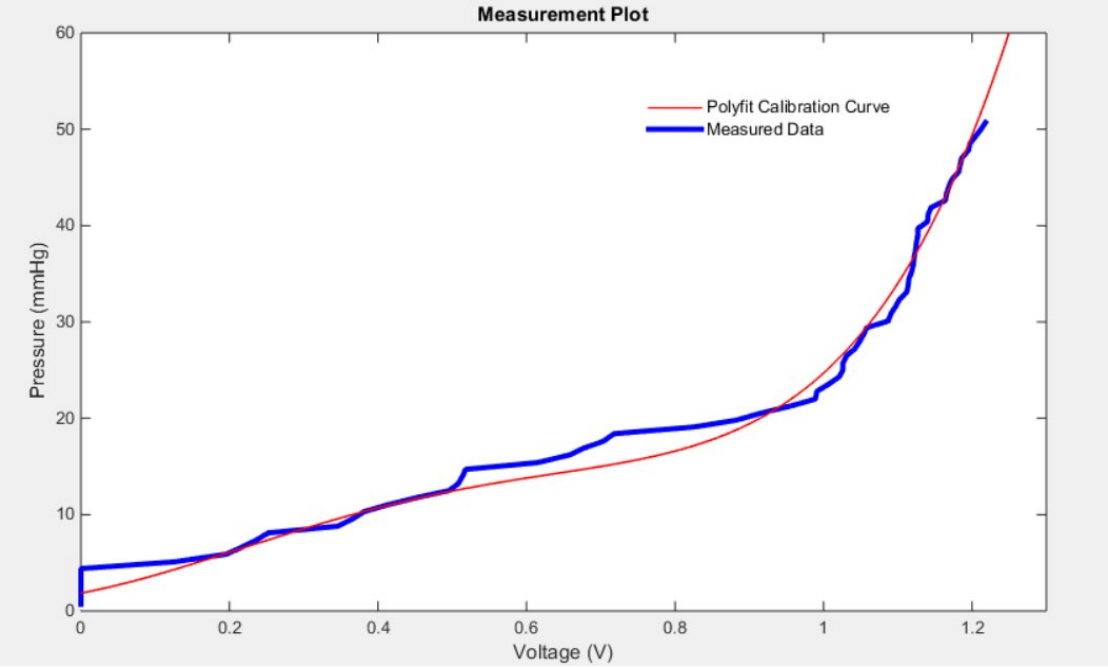

Figure 29. Voltage measurement plot of FSR

This plot represents the measured voltage versus the estimated pressure with the calibration curve.

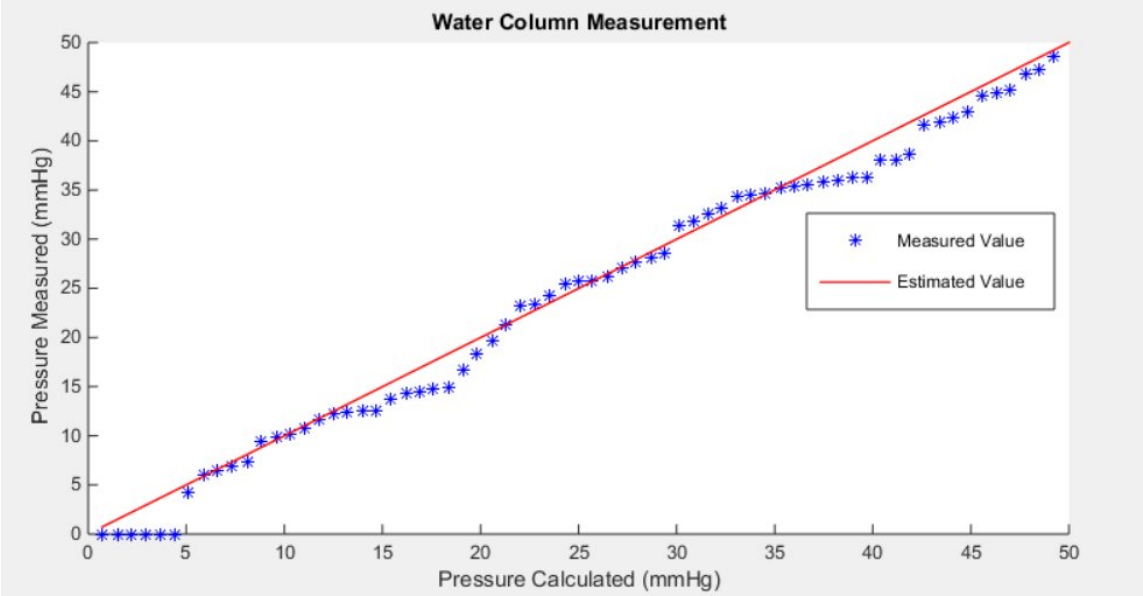

Figure 30. Measurement output plot of FSR

This plot represents the deviation of the pressure measurement from the actual value

Discussion

Force sensing resistors were fairly satisfactory in measuring and estimating the applied pressure. The commercial FSR with the standard spacer has lower limit of pressure sensitivity starting at 25.9 mmHg. With the spacer modification, the same FSR was able to detect pressure starting from 5.1mmHg. However, the AAMI standards for ICP monitoring demands the device dynamic requirement to be 0-100 mmHg. Since, the FSR with spacer modification has a limit of detection starting at 5.1 mmHg, this pressure transducing material cannot be used for an ICP sensing application. Nevertheless, if the sensitivity could be improved using a thinner spacer (<1.5mil), this could be used for ICP measurements provided the resolution and error characteristics of the transducer satisfy AAMI standards.

Further, part to part variability was magnified in the lower pressure range, which could be attributed to the non-uniform dispersion of pressure sensitive ink as the commercial preparation is not meant for low pressure application. Accounting to low sensitivity and high part to part variability, further experimentation with the FSR was suspended.

Bench Test - MEMS Piezoresistive Sensor

Calibration

Sensor Calibration:

The sensor was calibrated as per the manufacturer's recommended procedure by connecting 150kΩ resistor between the supply and the positive output pin. This provides an output voltage equivalent to 100 mmHg, which was 2.945 V for a supply voltage of

5.89V. The voltage divider was designed to provide 6V, but in practice it provided 5.89V. The sensor calibration factor / sensitivity was observed to be 5uV/V/mmHg, exactly following manufacturer's typically specification. The value was calculated as follows:

$$Sensitivity\ specified = 5\ \mu V/mmHg$$

$$Sensitivity\ observered\ (S) = \frac{5\ \mu V}{mmHg}; with\ a\ 60db\ amplifier \frac{5\ mV}{mmHg}$$

$$S = \frac{Output\ Voltage\ for\ 100\ mmHg}{Pressure * Supply\ Voltage} = \frac{2.945}{100 \times 5.89} = 5\ mV$$

$$=> Calibration\ factor = S \times 5.89 = 0.02945\ V/mmHg$$

So as calculated, 0.02945V/mmHg for the supply voltage provided is set as the calibration factor to convert the voltage observed into pressured measured by the sensor.

System Calibration:

This is performed with the water column to check the accuracy of the calibration factor. Four specific water levels (2 cm,4 cm,6 cm and 8 cm) are considered to provide pressure over the sensor. Each water level, i.e. pressure applied is repeated thrice to estimate the error due to calibration. The aim of this procedure was also to determine whether the sensor is sensitive below 5 mmHg as specified by the manufacturer.

Below is a table of the calibration measurements and observed voltage outputs after amplification.

Table 2

Tabulation of sensor output for system calibration

Height of Water in column (cm)	Pressure (mmHg)	Voltage V1 (V)	Voltage V2 (V)	Voltage V3 (V)	Averaged Voltage Observed (V)
2	1.5	0.0442	0.0434	0.0447	0.0441
4	2.9	0.0855	0.0864	0.0856	0.0858
6	4.4	0.127	0.131	0.132	0.13
8	5.1	0.172	0.171	0.175	0.173

Further, a calibration graph was plotted as shown below with the standard error at observed at that particular pressure.

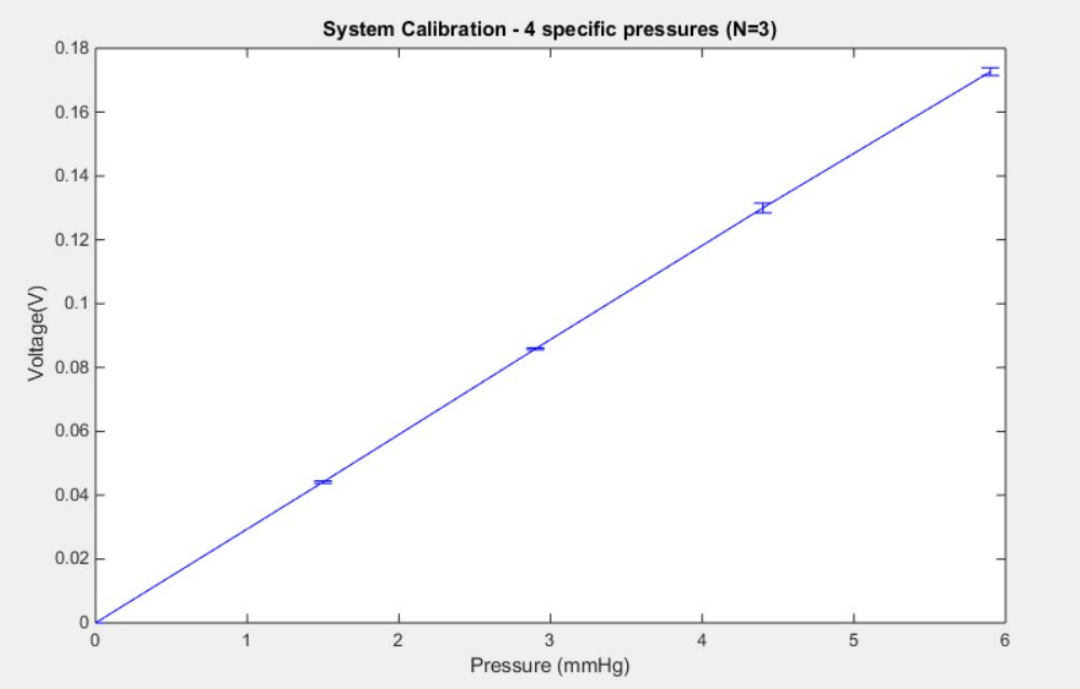

Figure 31. Standard error plot of system calibration.
This plot represents the standard error in measurement for the fixed calibration factor determined by sensor calibration.

An important process to note here is, the offset adjustment for the sensor is a manual intervention, which has significant control over the system reading and

calibration. So, this system calibration was repeated until the standard deviation was reduced to < 0.001V for all the specified pressures taken for observation.

Measurement

1) Static Test - Water column

The same setup was used after system calibration, ensuring no error was attributed due to setup changes. Pressures from 0-8.8 mmHg were applied in increments of 0.7 mmHg. Below is a plot of pressure measured versus the pressure estimated, showing the accuracy of the sensor.

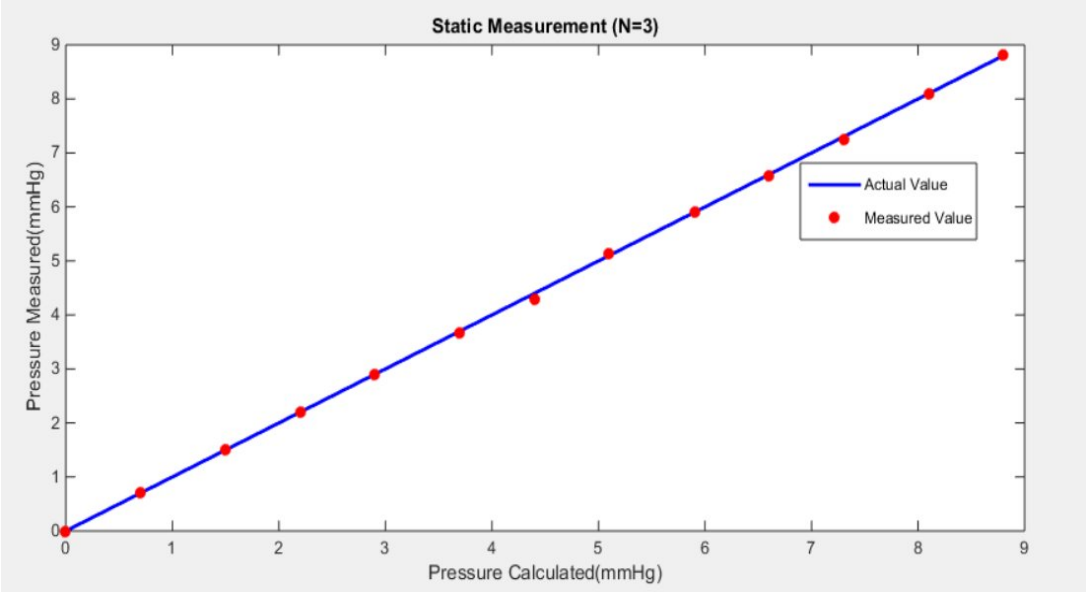

Figure 32. Static pressure measurement plot
This plot of pressure measured versus the actual pressure, representing the accuracy of the sensor for static measures

2) Dynamic Test - Air Pump

In this test, manually pumping a bulb provided the estimated pressure over the sensing area. This test involved approximation errors, since the procedure was to

manually pump the air to a certain pressure and at no point it was guaranteed that applied pumped pressure exactly reached the estimated pressure. The estimated pressure is determined by a pressure gauge with a resolution of 2 mmHg, indicating there could be an error of ± 2 mmHg in the applied pressure with respect to the pressure estimated.

The overall goal of this test was to qualitatively estimate the dynamic response of the sensor, i.e. if it measures pressure without any significant delay in the response. Applied pressure varied from 0-10 mmHg by manual pumping of air with an aim of providing at least two pumps per second. The figure below shows the output pressure measured inthis experiment.

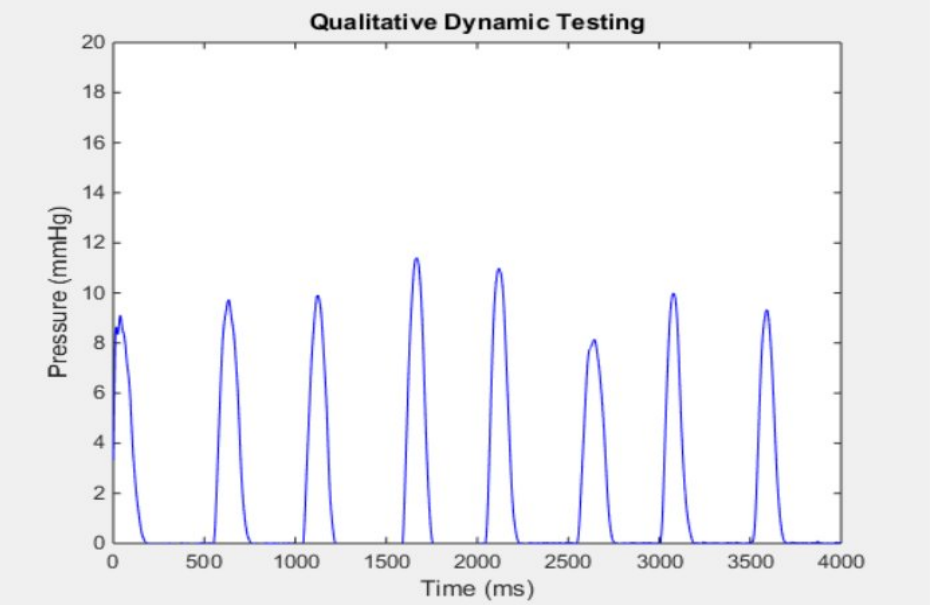

Figure 33. Dynamic pressure measurement plot showing the dynamic response of the sensor for a manually varied pressure over 4 seconds.

3) Media Test

This test was a static measurement that involved a liquid of different density and conductivity than water. This was performed as a conformational test before animal model testing due to similar media environment. Phosphate buffer saline was used as a

physiological media equivalent to perform this test. The pressure was varied from 0-8.8 mmHg and the figure below shows the response of the sensor for this experiment.

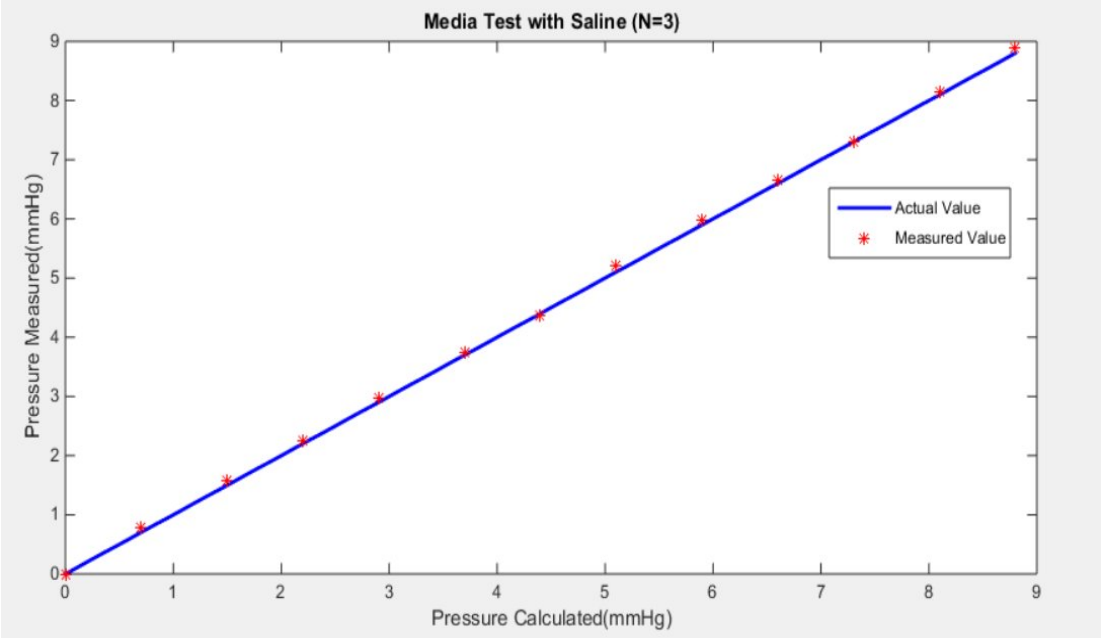

Figure 34. Static pressure measurement plot with saline media.

Discussion

This MEMS sensor, having dynamic range -30 to 300 mmHg is greatly accurate for an ICP application considered. The efficacy of the sensor ensured by the existing commercial application of this sensor for invasive blood pressure monitoring. However, the experimental setup, calibration and measurement were performed to estimate the error and offset adjustment required with the readout electronics used in our system before implementation in an animal model for ICP monitoring. The sensor after system calibration and adjustments, had a 0.1 mmHg accuracy on the benchtop, 2% error, 0.01 mmHg resolution and 0.1 mmHg precision.

The characteristics of the sensor were excellent for ICP monitoring and further experimentation with this sensor continued with the animal model implantation.

CHAPTER 6

RESULTS AND DISCUSSION

The animal study involved observing the baseline ICP, mechanically varying the ICP by abdominal compressions and varying the ICP by physiological perturbations with injections capable of resulting in a tonicity changes.

The experiment was conducted following the IACUC guidelines and approved protocol. Real time data observation determined the successful implantation of the sensor to the desired level of penetration or depth below the skull while remaining above the dura. As soon as the sensing cup was placed with its opening inside the skull over the drilled open area, a baseline ICP signal was observed which correlated with the heart rate at that point of time. This confirmed the implantation location and depth was appropriate for ICP measurements. After proper placement was confirmed, the sensing cup was sealed on to the skull to avoid fluid leakage and to obtain steady state conditions for accurate pressure measurements.

1) Real-Time Baseline ICP

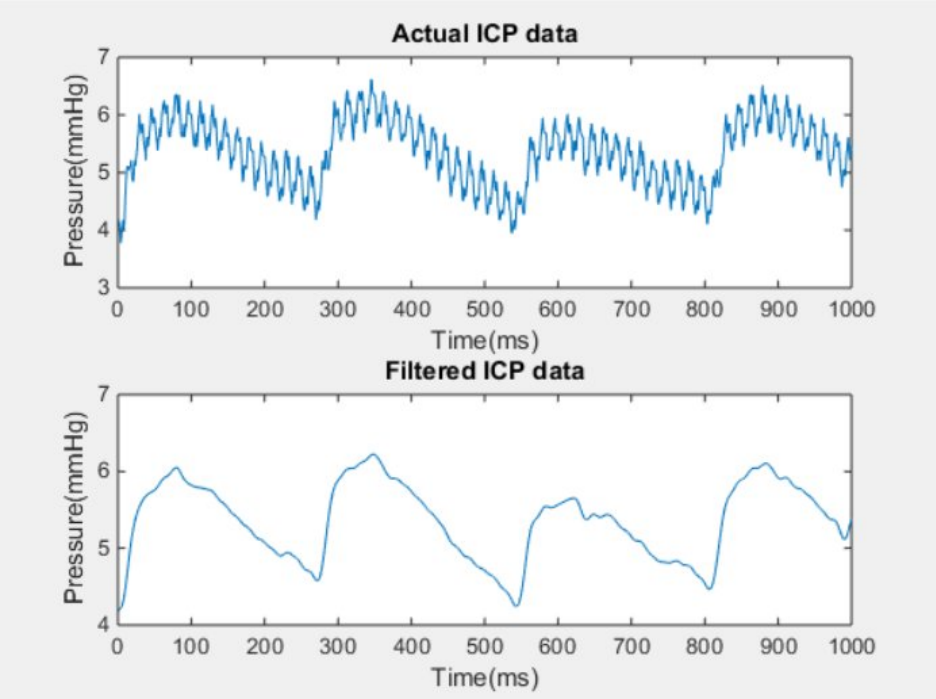

Figure 35. Baseline ICP, before and after filtering

The figure above shows the baseline ICP measured over one second, in which 60 Hz noise is observable in real-time, unfiltereddata. The raw signal with power line interference was filtered using a Butterworth low pass filter with a cutoff frequency of 30Hz. The average heart rate of a rat ranges from 240-490/minute, which translates to 4-8.1 Hz. These low frequency components are dominant signal observed.

2) Analysis Plots

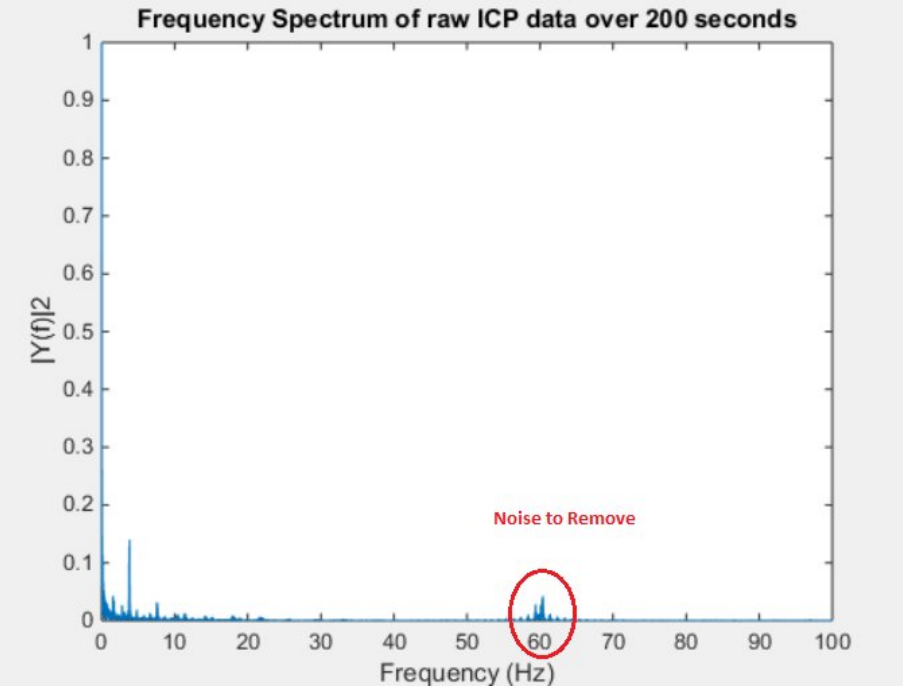

Figure 36. FFT of the ICP signal before filtering

The above figure is a plot of the frequency spectrum of the measured ICP signal. The plot has clearly observable noise components and lower frequency components (including DC), which are our signals of interest. This spectrum is generated from 200 seconds data that covers a range of heart rates from 199-255 bpm. Due to heart rate variability, we observed a set of low peaks around 4-5 Hz.

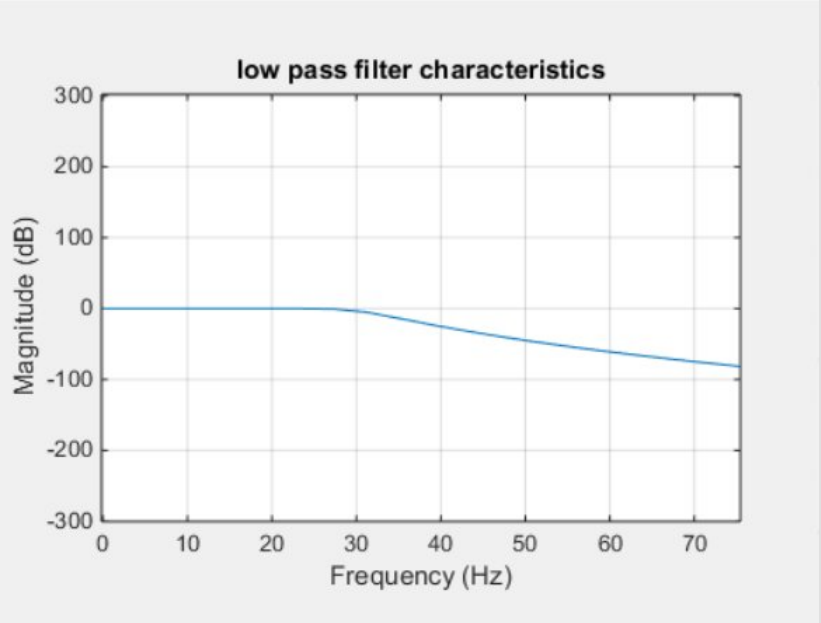

Figure 37. Filter characteristics of a Butterworth filter

The above figure represents the 30Hz cutoff implemented using a 10th order digital Butterworth filter.

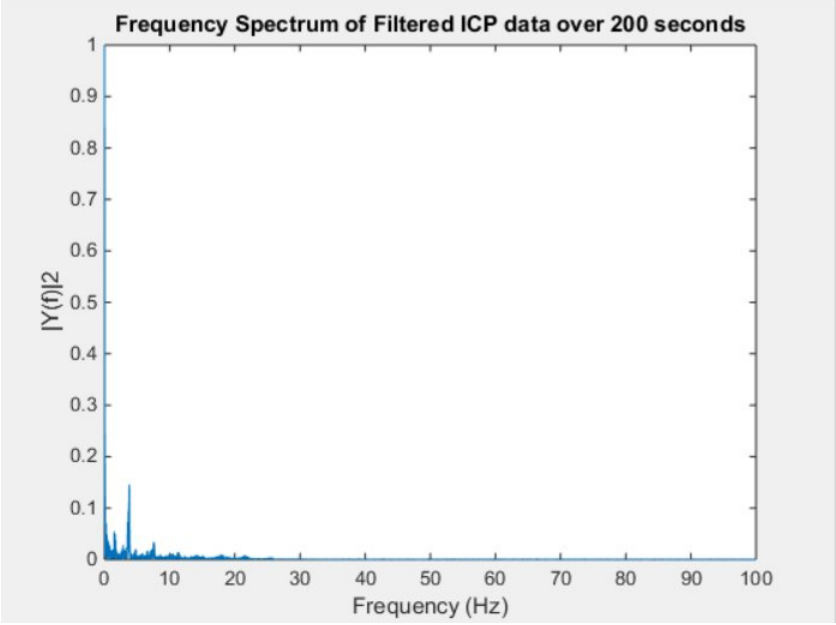

Figure 38. FFT of the ICP signal after filtering

The above figure is plotted to confirm the noise above 30 Hz is removed

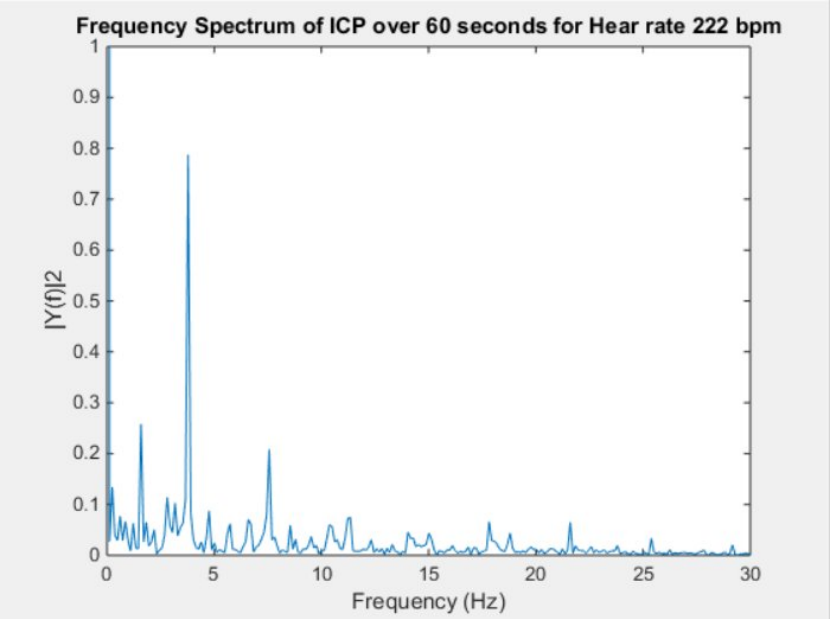

Figure 39. FFT of the ICP signal at a certain heart rate

This plot shows the frequency peak correlating to the heart rate observed at that time, which clearly indicates a good signal strength.

3) Baseline intracranial pressure data for over one second

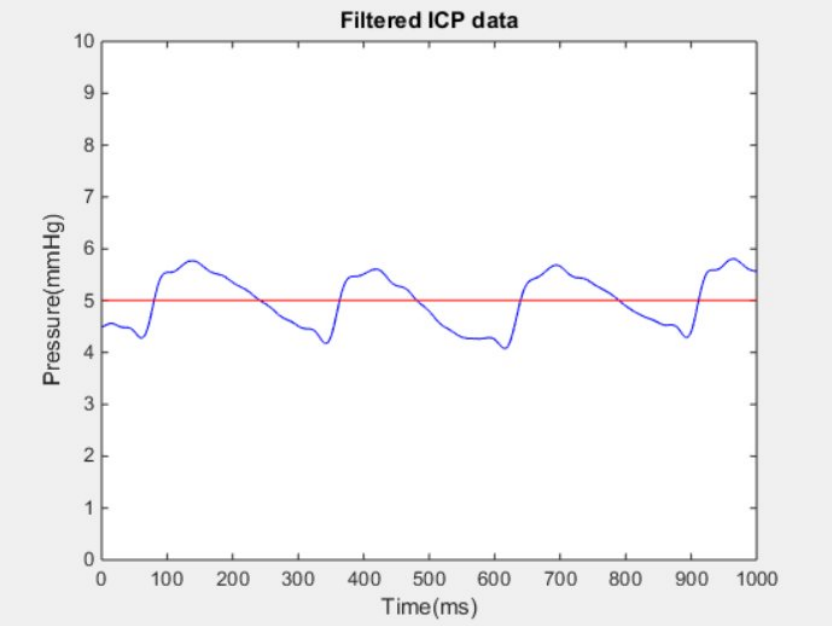

Figure 40. Baseline ICP for heart rate of 220 bpm

The ICP signal's magnitude or DC content represented the baseline pressure inside the rat's brain at any given instance in time. The frequency of the ICP signal follows and correlates with the heart rate at that point, which is 220 bpm in this case.

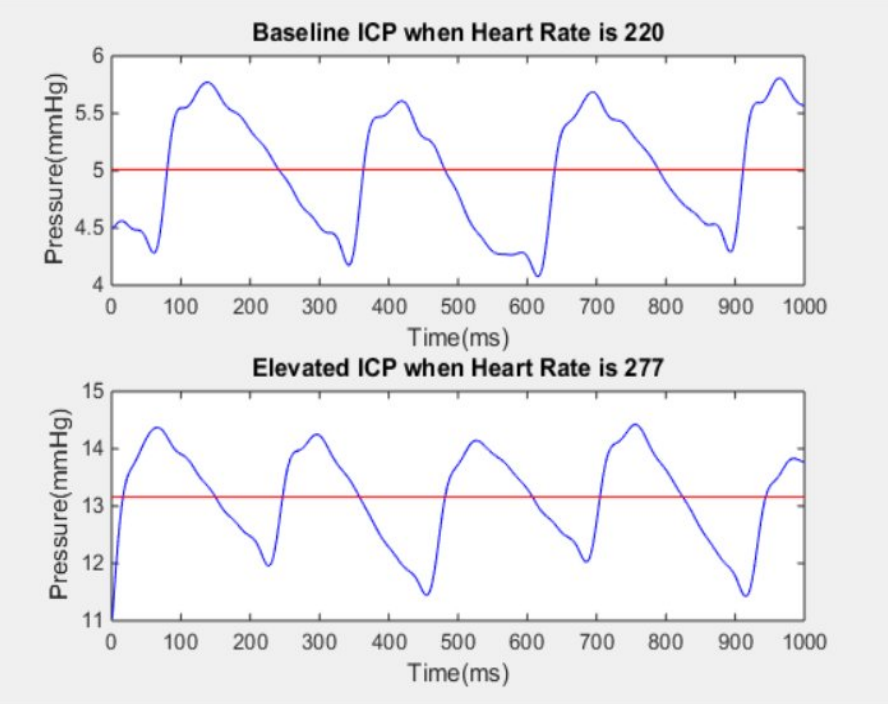

Figure 41. ICP over one second at different physiological conditions

4) Experimental Perturbation Data

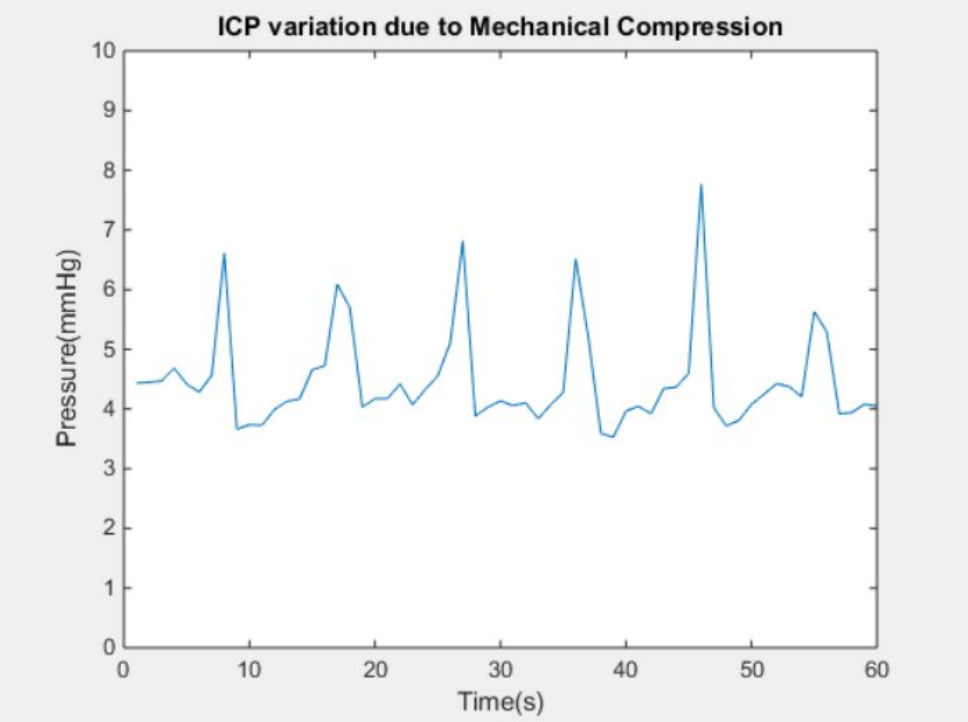

Figure 42. ICP variation due to Mechanical Compression

A manual mechanical compression procedure was used to vary the ICP. The target was to provide compression every 10 seconds, however manual variations and reaction time is observable in the timing of compression and relaxation. The plot above shows a great correlation in ICP for mechanical compression and relaxation protocol.

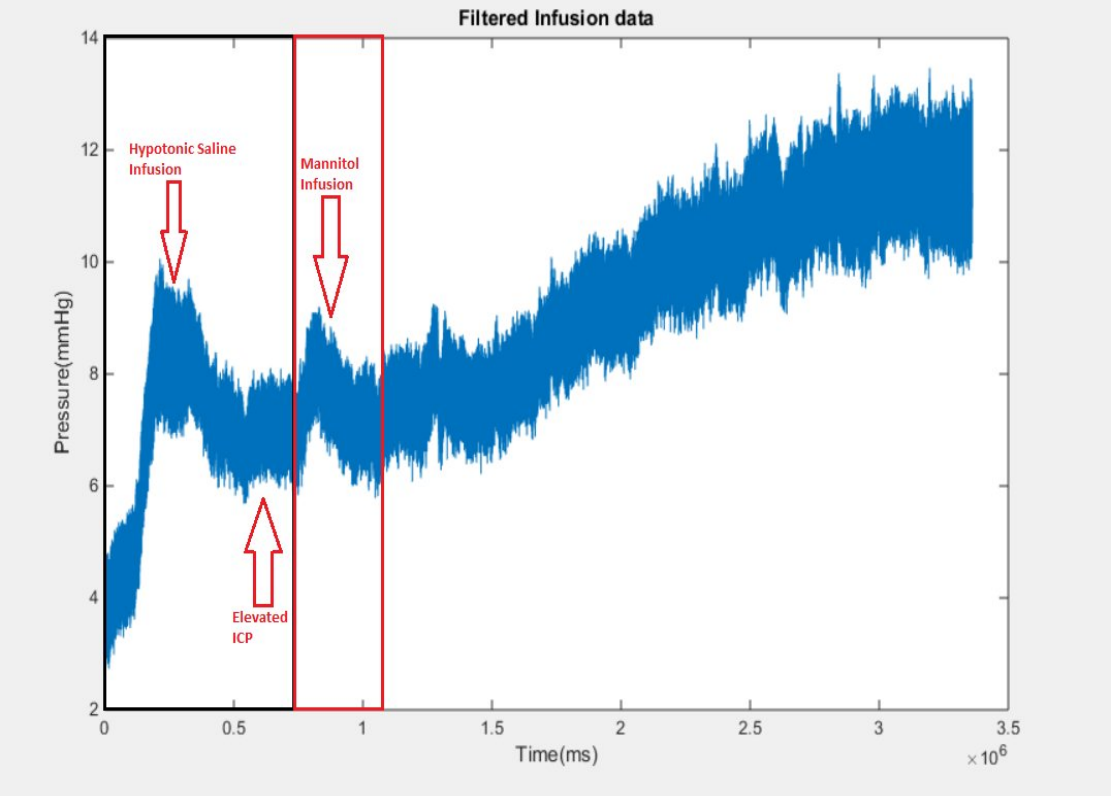

Figure 43. Filtered infusion data

The above figure shows the overall experimental infusion cue. The peaks correlate with the injection times and in turn serve as a visual indicator of the physiological changes.

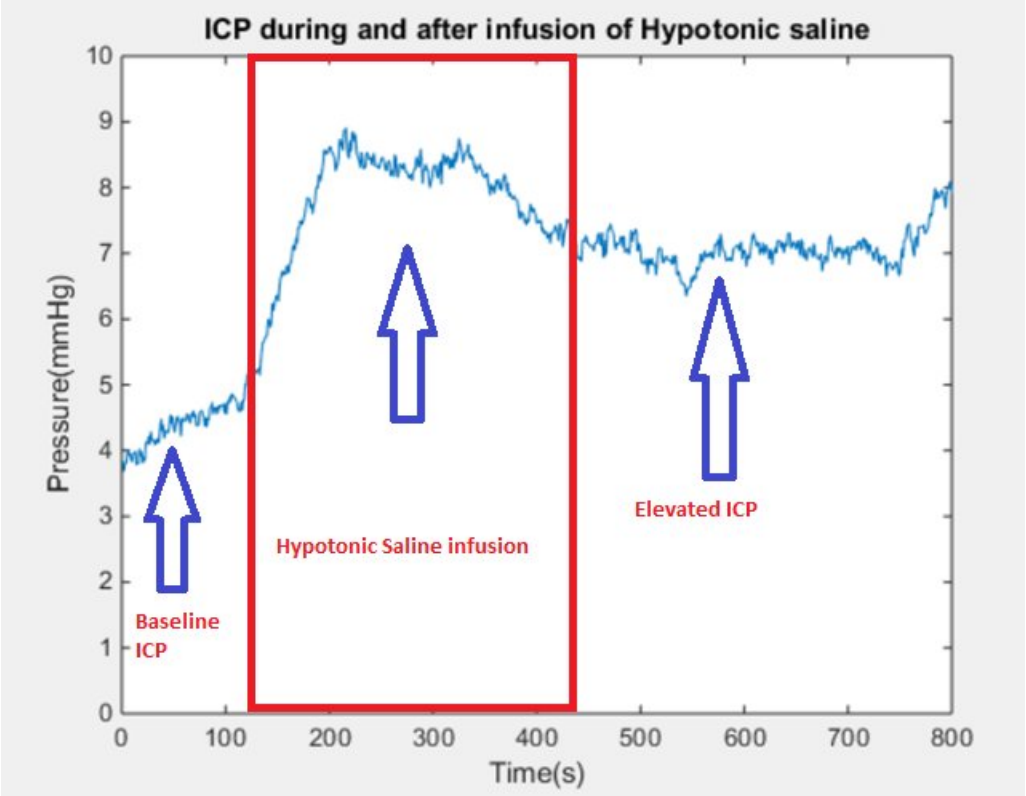

Figure 44. Hypotonic saline injection and elevation in ICP

As seen in the figure above, after injection of hypotonic saline, there is an increase in the baseline ICP level. This demonstrates the responsivity and efficacy of the system.

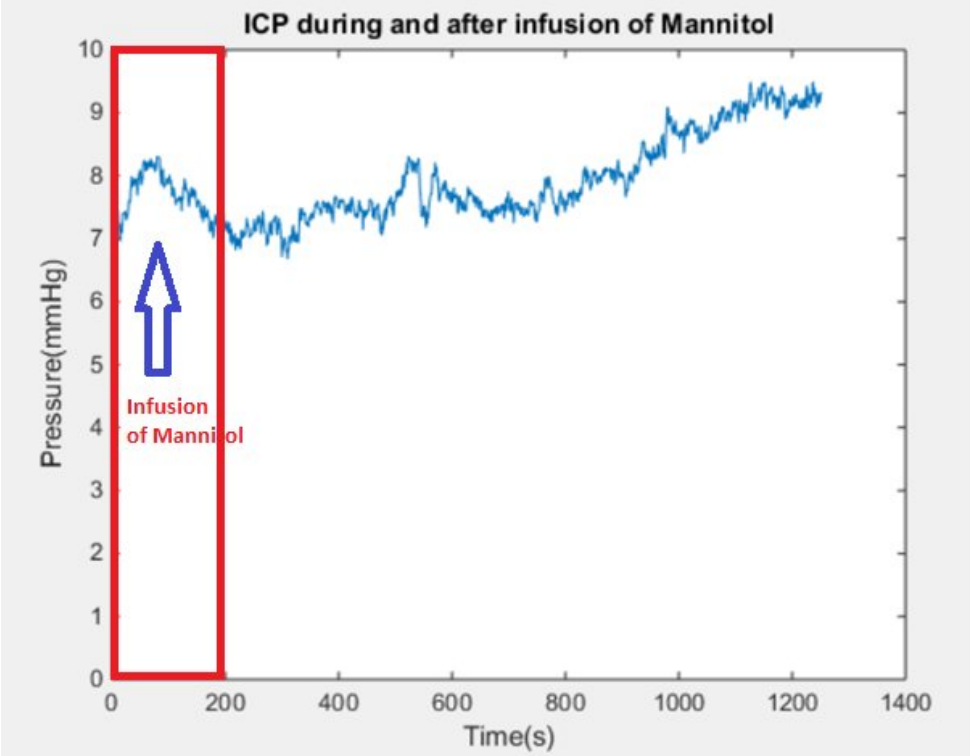

Figure 45. Mannitol injection results

Mannitol was expected to lower ICP, but instead ICP increased. ICP neither returned to baseline nor decrease. While we can only make conjectures as to the cause of this behavior, we can offer two hypotheses:

1) Hypotonic saline volume injected was too high, elevating the ICP much more than the level expected. Due to this large volume, the ICP could no longer be reduced with Mannitol infusion. Additionally, the volume is increased with any infusion and this could actually be increasing ICP further

2) Effective time for mannitol to decrease the pressure might be several hours, which was out of our range of experimentation time that we could not observe any response.

Discussion

The results of the animal model experiments provided confidence that we can use this system to observe ICP. With the exception of mannitol infusion, which did not produce the desired effect of decreasing ICP, the functioning of the system was highly satisfactory and as expected. Nevertheless, after euthanasia, the varying pressure waves disappeared and just a baseline static pressure was observed. This stated that sensor was still working great after mannitol infusion. The aim of evaluation and testing the efficacy of the system was accomplished. The system had good accuracy and repeatability in measuring ICP without any significant delay.

Interestingly, the real-time ICP signal had a very high power line noise, although the whole system was battery powered. It is suspected that the noise coupled from the pulse oximeter probe attached to the rat's foot for measuring the vital parameters during the surgery. Another exciting observation was that, ICP monitor was faster in detecting any changes in heart rate or reaction to changes in anesthesia settings, than the pulse oximeter. These real time observation further justify the system functionality and bolster its potential as ICP monitor.

CHAPTER 7

CONCLUSION AND FUTURE SCOPE

Intracranial pressure was successfully monitored and analyzed in rats, by our epidural ICP monitoring system.

This ICP monitoring system was designed using a commercially available pressure transducer intended for biomedical applications. This transducer is a disposable blood pressure sensor used in extra vascular catheters for invasive blood pressure monitoring. This sensor was adapted to develop an epidural ICP monitoring system due to the characteristics of the sensor that were well matched with the requirement. After the system design, calibration and successful bench testing, the system was taken for the next level of testing in animal model - *rattus norvegicus* (Rat).

The result from the rat model showed the efficacy of the sensor for an epidural ICP application and demonstrated this system can continuously measure ICP. The ICP signal observed had good correlation with the physiology. The signal clearly had a baseline ICP value and its frequency correlated with the heart rate at that instance, throughout the experiment, which is a typical characteristic of an ICP signal. The results of ICP variations induced by mechanical compressions of the abdomen or by involvement of physiological drug infusion, served as an evidence that this system could potentially detect ICP variations accurately, repeatably and without any significant delays involved.

Further, the system followed the AAMI standard specification for intracranial pressure monitoring viz:

1) Dynamic pressure measurement range of 0-100 mmHg

2) Accuracy of ±2 mmHg in 0-20 mmHg range

3) 10% maximum error in 20-100 mmHg range

Thus, this research work is a proof of concept for a monitoring system that could provide a minimally invasive, highly accurate ICP recordings. This work also sets the stage for an integrated system design.

The sensor uses a MEMS die that acts as a strain gauge and measures the pressure changes. With integrated electronics and MEMS technology, this die could be embedded as a chip on an ECoG electrode array, which would be an elegant and highly effective solution to monitoring brain pressure in the presence of brain implants or electrodes.

Further, this technology is a simple and lower cost than any of the commercially existing intracranial pressure monitoring systems available in the market today. Thus we believe this system has the potential to transform monitoring of intracranial pressure for both minimally invasive monitoring and ECoG applications

REFERENCES

[1]"Statistics on TBI" US Centers for Disease Control and Prevention. Web:<http://www.cdc.gov/traumaticbraininjury/pdf/BlueBook_factsheet-a.pdf>

[2] Raboel, P. H., et al. "Intracranial pressure monitoring: invasive versus non-invasive methods—a review." *Critical care research and practice* 2012 (2012).

[3] Pattinson, Kyle, Guy Wynne-Jones, and Christopher HE Imray. "Monitoring intracranial pressure, perfusion and metabolism." *Continuing Education in Anaesthesia, Critical Care & Pain* 5.4 (2005): 130-133.

[4] Czosnyka, Marek, and John D. Pickard. "Monitoring and interpretation of intracranial pressure." *Journal of Neurology, Neurosurgery & Psychiatry* 75.6 (2004): 813-821.

[5] Matsushita, Kojiro, et al. "Development of an implantable wireless ECoG 128ch recording device for clinical brain machine interface." *Engineering in Medicine and Biology Society (EMBC), 2013 35th Annual International Conference of the IEEE*. IEEE, 2013.

[6] Hirata, Masayuki, et al. "A fully-implantable wireless system for human brain-machine interfaces using brain surface electrodes: W-HERBS." *IEICE transactions on communications* 94.9 (2011): 2448-2453.

[7] Anderson, Grant S., and Reid R. Harrison. "Wireless integrated circuit for the acquisition of electrocorticogram signals." *Circuits and Systems (ISCAS), Proceedings of 2010 IEEE International Symposium on*. IEEE, 2010.

[8] Chang, Chih-Wei, and Jin-Chern Chiou. "A wireless and batteryless microsystem with implantable grid electrode/3-dimensional probe array for ECoG and extracellular neural recording in rats." *Sensors* 13.4 (2013): 4624-4639.

[9] Wang, Po T., et al. "A co-registration approach for electrocorticogram electrode localization using post-implantation MRI and CT of the head." *Neural Engineering (NER), 2013 6th International IEEE/EMBS Conference on*. IEEE, 2013.

[10] Charvet, G., et al. "A wireless 64-channel ECoG recording electronic for implantable monitoring and BCI applications: WIMAGINE." *Engineering in Medicine and Biology Society (EMBC), 2012 Annual International Conference of the IEEE*. IEEE, 2012.

[11] Speck, Verena, et al. "Lumbar catheter for monitoring of intracranial pressure in patients with post-hemorrhagic communicating hydrocephalus." *Neurocritical care* 14.2 (2011): 208-215.

[12] N. KAPADIA, AN JHA, F. "Simultaneous lumbar and intraventricular manometry to evaluate the role and safety of lumbar puncture in raised intracranial pressure following subarachnoid haemorrhage." *British journal of neurosurgery* 10.6 (1996): 585-588.

[13] Lenfeldt, Niklas, et al. "CSF pressure assessed by lumbar puncture agrees with intracranial pressure." *Neurology* 68.2 (2007): 155-158.

[14] Smith, Martin. "Monitoring intracranial pressure in traumatic brain injury."*Anesthesia & Analgesia* 106.1 (2008): 240-248.

[15] Zhong, Jun, et al. "Advances in ICP monitoring techniques." *Neurological research* 25.4 (2003): 339-350.

[16] March, Karen. "Intracranial pressure monitoring: why monitor?." *AACN Advanced Critical Care* 16.4 (2005): 456-475.

[17] Steiner, L. A., and P. J. D. Andrews. "Monitoring the injured brain: ICP and CBF." *British journal of anaesthesia* 97.1 (2006): 26-38.

[18] Bhatia, Anuj, and Arun Kumar Gupta. "Neuromonitoring in the intensive care unit. I. Intracranial pressure and cerebral blood flow monitoring." *Intensive care medicine* 33.7 (2007): 1263-1271.

[19] Binz, Daniel D., L. Gerard Toussaint III, and Jonathan A. Friedman. "Hemorrhagic complications of ventriculostomy placement: a meta-analysis."*Neurocritical care* 10.2 (2009): 253-256.

[20] Beer, R., et al. "Nosocomial ventriculitis and meningitis in neurocritical care patients." *Journal of neurology* 255.11 (2008): 1617-1624.

[21] Hoefnagel, D., et al. "Risk factors for infections related to external ventricular drainage." *Acta neurochirurgica* 150.3 (2008): 209-214.

[22] Brain, Trauma Foundation. "Guidelines for the management of severe traumatic brain injury. IV. Infection prophylaxis." *Journal of neurotrauma* 24 (2007): S26.

[23] Lozier, Alan P., et al. "Ventriculostomy-related infections: a critical review of the literature." *Neurosurgery* 51.1 (2002): 170-182

[24] Fichtner, Jens, et al. "Efficacy of silver-bearing external ventricular drainage catheters: a retrospective analysis: Clinical article." *Journal of neurosurgery*112.4 (2010): 840-846.

[25] O'Neill, Brent R., et al. "A survey of ventriculostomy and intracranial pressure monitor placement practices." *Surgical neurology* 70.3 (2008): 268-273.

[26] O'Leary, Shaun T., et al. "Efficacy of the Ghajar Guide revisited: a prospective study." *Journal of neurosurgery* 92.5 (2000): 801-803.

[27] Drake, J. M. "Ventriculostomy for treatment of hydrocephalus." *Neurosurgery Clinics of North America* 4.4 (1993): 657-666.

[28] North, Brian, and Peter Reilly. "Comparison among three methods of intracranial pressure recording." *Neurosurgery* 18.6 (1986): 730-732.

[29] Bruder, N., et al. "A comparison of extradural and intraparenchymatous intracranial pressures in head injured patients." *Intensive care medicine* 21.10 (1995): 850-852.

[30] Eide, Per Kristian. "Comparison of simultaneous continuous intracranial pressure (ICP) signals from ICP sensors placed within the brain parenchyma and the epidural space." *Medical engineering & physics* 30.1 (2008): 34-40.

[31] Weinstabl, Christian, et al. "Comparative analysis between epidural (Gaeltec) and subdural (Camino) intracranial pressure probes." *Journal of clinical monitoring* 8.2 (1992): 116-120.

[32] Poca, Maria Antonia, et al. "Is intracranial pressure monitoring in the epidural space reliable? Fact and fiction." *Journal of neurosurgery* 106.4 (2007): 548-556.

[33] Gelabert-Gonzalez, M., et al. "The Camino intracranial pressure device in clinical practice. Assessment in a 1000 cases." *Acta neurochirurgica* 148.4 (2006): 435-441.

[34] Bekar, A., et al. "Risk factors and complications of intracranial pressure monitoring with a fiberoptic device." *Journal of Clinical Neuroscience* 16.2 (2009): 236-240.

[35] Hong, Wei-Chen, et al. "Subdural intracranial pressure monitoring in severe head injury: clinical experience with the Codman MicroSensor." *Surgical neurology* 66 (2006): S8-S13.

[36] Koskinen, Lars-Owe D., and Magnus Olivecrona. "Clinical experience with the intraparenchymal intracranial pressure monitoring Codman MicroSensor system." *Neurosurgery* 56.4 (2005): 693-698.

[37] Citerio, Giuseppe, et al. "Multicenter Clinical Assessment of the Raumedic Neurovent-P Intracranial Pressure Sensor: A Report By the Brainit Group."*Neurosurgery* 63.6 (2008): 1152-1158.

[38] Lescot, Thomas, et al. "In vivo accuracy of two intraparenchymal intracranial pressure monitors." *Applied Physiology in Intensive Care Medicine 1*. Springer Berlin Heidelberg, 2012. 249-253.

[39] Allin, David, Marek Czosnyka, and Zofia Czosnyka. "Laboratory testing of the Pressio intracranial pressure monitor." *Neurosurgery* 62.5 (2008): 1158-1161

[40] Lang, Josef-Michael, et al. "Clinical evaluation of intraparenchymal Spiegelberg pressure sensor." *Neurosurgery* 52.6 (2003): 1455-1459.

[41] Kiening, K. L., et al. "Continuous monitoring of intracranial compliance after severe head injury: relation to data quality, intracranial pressure and brain tissue PO2." *British journal of neurosurgery* 17.4 (2003): 311-318.

[42] Kiening, K. L., et al. "Assessment of the relationship between age and continuous intracranial compliance." *Intracranial Pressure and Brain Monitoring XII*. Springer Vienna, 2005. 293-297.

[43] Shellock, Frank G. "Biomedical implants and devices: Assessment of magnetic field interactions with a 3.0-Tesla MR system." *Journal of Magnetic Resonance Imaging* 16.6 (2002): 721-732.

[44] Stendel, R., et al. "Clinical evaluation of a new intracranial pressure monitoring device." *Acta neurochirurgica* 145.3 (2003): 185-193.

[45] Bellner, Johan, et al. "Transcranial Doppler sonography pulsatility index (PI) reflects intracranial pressure (ICP)." *Surgical neurology* 62.1 (2004): 45-51.

[46] Moreno, José A., et al. "Evaluating the outcome of severe head injury with transcranial Doppler ultrasonography." *Neurosurgical focus* 8.1 (2000): 1-7.

[47] Voulgaris, Spyridon G., et al. "Early cerebral monitoring using the transcranial Doppler pulsatility index in patients with severe brain trauma." *Annals of Transplantation* 11.2 (2005): CR49-CR52.

[48] Behrens, Anders, et al. "Transcranial Doppler pulsatility index: not an accurate method to assess intracranial pressure." *Neurosurgery* 66.6 (2010): 1050-1057.

[49] Brandi, Giovanna, et al. "Transcranial color-coded duplex sonography allows to assess cerebral perfusion pressure noninvasively following severe traumatic brain injury." *Acta neurochirurgica* 152.6 (2010): 965-972.

[50] Reid, A., et al. "The relationship between intracranial pressure and tympanic membrane displacement." *British journal of audiology* 24.2 (1990): 123-129.

[51] Shimbles, S., et al. "Clinical comparison of tympanic membrane displacement with invasive intracranial pressure measurements." *Physiological measurement*26.6 (2005): 1085.

[52] Kimberly, Heidi Harbison, et al. "Correlation of optic nerve sheath diameter with direct measurement of intracranial pressure." *Academic Emergency Medicine*15.2 (2008): 201-204.

[53] Rajajee, Venkatakrishna, et al. "Optic nerve ultrasound for the detection of raised intracranial pressure." *Neurocritical care* 15.3 (2011): 506-515.

[54] Bäuerle, Jochen, et al. "Intra-and Interobsever Reliability of Sonographic Assessment of the Optic Nerve Sheath Diameter in Healthy Adults." *Journal of Neuroimaging* 22.1 (2012): 42-45.

[55] Marshall, I., et al. "Assessment of factors affecting MRI measurement of intracranial volume changes and elastance index." *British journal of neurosurgery* 22.3 (2008): 389-397.

[56] Dunn, Laurence T. "Raised intracranial pressure." *Journal of Neurology, Neurosurgery & Psychiatry* 73.suppl 1 (2002): i23-i27.

[57] Lemaire, J. J., et al. "Slow pressure waves in the cranial enclosure." *Acta neurochirurgica* 144.3 (2002): 243-254.

[58] Yaniger, S. I. "Force sensing resistors: A review of the technology." *Electro International, 1991*. IEEE, 1991.

[59] Hollinger, Avrum, and Marcelo M. Wanderley. "Evaluation of commercial force-sensing resistors." *Proceedings of International Conference on New Interfaces for Musical Expression*. 2006.

[60] Eventoff, Franklin N. "Pressure transducer." U.S. Patent No. 4,314,228. 2 Feb. 1982.

[61] Ferguson-Pell, Martin, Satsue Hagisawa, and Duncan Bain. "Evaluation of a sensor for low interface pressure applications." *Medical engineering & physics*22.9 (2000): 657-663

[62] Flórez, J. A., and A. Velasquez. "Calibration of force sensing resistors (fsr) for static and dynamic applications." *ANDESCON, 2010 IEEE*. 2010.

[63] Meng, Xu, et al. "Dynamic evaluation of a digital wireless intracranial pressure sensor for the assessment of traumatic brain injury in a swine model."*Microwave Theory and Techniques, IEEE Transactions on* 61.1 (2013): 316-325.

[64] "Camino Pressure Sensor Product Models" Integra Life. Web <http://www.integralife.com/products%2FPDFs%2FNeuroCriticalCare%2FCamino%20Brochure.pdf>

[65] "Codman ICP Monitoring System" DePuy Synthes. Web <https://emea.depuysynthes.com/hcp/codman-neuro/products/qs/icp-monitoring-system>

[66] " Intracranial Pressure Monitoring" Speigelberg. Web<http://www.spiegelberg.de/>

[67] " FSR 101 - The Basics" Sensitronics LLC. Web<http://sensitronics.com/fsr101.htm>

[68] "1620 MEMS Blood Pressure Sensor: Measurement Specialties. Web<http://www.meas-spec.com/downloads/1620.pdf>

[69] "Membrane Switch Spacers" Solutions 3M. Web<http://multimedia.3m.com/mws/media/66424O/3mtm-200mp-membrane-switch.pdf>

[70] "Single Zone Sensors" Sensitronics LLC. Web <http://sensitronics.com/products-1-inch-thru-mode-fsr.php>

[71] "Instrumentation Amplifier INA 101" Burr Brown. Web<http://pdf.datasheetcatalog.com/datasheet/BurrBrown/mXryuyt.pdf>

[72] Clasa Anesthesia. Web< http://www.clasa-anestesia.org/revistas/argentina/HTML/ArgMonitoreo_Neurolgico.htm >

APPENDIX A

IACUC PROTOCOL APPROVAL AND AMMENDEMENT

Institutional Animal Care and Use Committee (IACUC)
Office of Research Integrity and Assurance
Arizona State University
660 South Mill
Avenue, Suite 315
Tempe, Arizona
85287-6111
Phone: (480) 965-4387 *FAX:* (480) 965-7772

Animal Protocol Review

ASU Protocol Number:	**15-1420R**
Protocol Title:	**Intracranial Pressure Monitoring**
Principal Investigator:	**Jennifer Blain Christen**
Date of Action:	**2/26/2015**

The animal protocol review was considered by the Committee and the following decisions were made:

The protocol was approved as modified.

If you have not already done so, documentation of Level III Training (i.e., procedure-specific training) will need to be provided to the IACUC office before participants can perform procedures independently. For more information on Level III requirements see https://researchintegrity.asu.edu/training/animals/levelthree.

Total # of Animals:	**5**	
		Pain Level:
Species:	**Rats**	**D**
Protocol Approval Period:	**2/26/2015 – 2/25/2018**	
Sponsor:	**N/A**	
ASU Proposal/Award #:	**N/A**	
Title:	**N/A**	

Signature: Augustowski for C. Johnson Date: 3/4/2015
IACUC Chair or

Institutional Animal Care and Use Committee (IACUC)
Office of Research Integrity and Assurance
Arizona State University
660 South Mill
Avenue, Suite 315
Tempe, Arizona
85287-6111
Phone: (480) 965-4387 *FAX:* (480) 965-7772

Animal Protocol Review

ASU Protocol Number:	**15-1420R Amendment #1**
Protocol Title:	**Intracranial Pressure Monitoring**
Principal Investigator:	**Jennifer Blain Christen**
Date of Action:	**3/6/2015**

The animal protocol review was considered by the Committee and the following decisions were made:

The amendment was approved by Designated Review to allow for single housing and to change Dr. Jennifer Blain Christen's role in the protocol.

If you have not already done so, documentation of Level III Training (i.e., procedure-specific training) will need to be provided to the IACUC office before participants can perform procedures independently. For more information on Level III requirements see https://researchintegrity.asu.edu/training/animals/levelthree.

Total # of Animals:	**5**	
		Pain Level:
Species:	**Rats**	**D**
Protocol Approval Period:	**2/26/2015 – 2/25/2018**	
Sponsor:	**N/A**	
ASU Proposal/Award #:	**N/A**	
Title:	**N/A**	

ignature: Augustowski for C. Johnson Date: 3/6/2015
IACUC Chair or

Institutional Animal Care and Use Committee (IACUC)
Office of Research Integrity and Assurance
Arizona State University
660 South Mill
Avenue, Suite 315
Tempe, Arizona
85287-6111
Phone: (480) 965-4387 *FAX:* (480) 965-7772

Animal Protocol Review

ASU Protocol Number:	**15-1420R Amendment #2**
Protocol Title:	**Intracranial Pressure Monitoring**
Principal Investigator:	**Jennifer Blain Christen**
Date of Action:	**3/9/2015**

The animal protocol review was considered by the Committee and the following decisions were made:

The amendment was administratively approved to allow for the one time change in drugs used to decrease intracranial pressure.

If you have not already done so, documentation of Level III Training (i.e., procedure-specific training) will need to be provided to the IACUC office before participants can perform procedures independently. For more information on Level III requirements see https://researchintegrity.asu.edu/training/animals/levelthree.

Total # of Animals:	**5**	
		Pain Level:
Species:	**Rats**	**D**
Protocol Approval Period:	**2/26/2015 – 2/25/2018**	
Sponsor:	**N/A**	
ASU Proposal/Award #:	**N/A**	
Title:	**N/A**	

Signature: 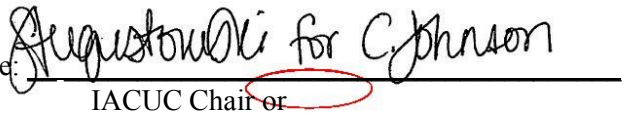 Date: 3/13/2015
IACUC Chair or

APPENDIX B

PHOTOGRAPH OF PROTOTYPING, DEVELOPED SYSTEM, BENCH TESTING SET UP AND ANIMAL MODEL IMPLANTATION

Sensing cup dimensions:

Sensing cup sealed onto the sensor

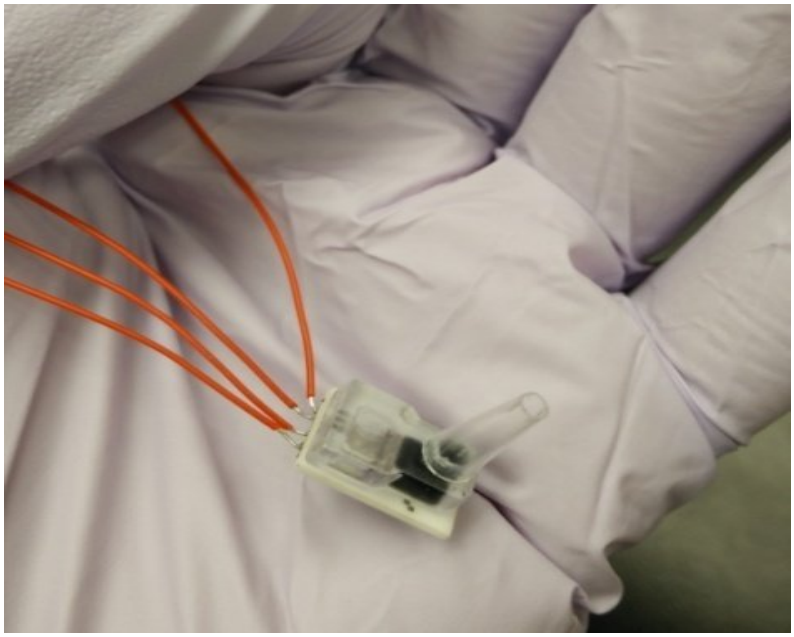

Prototyped and packaged circuit

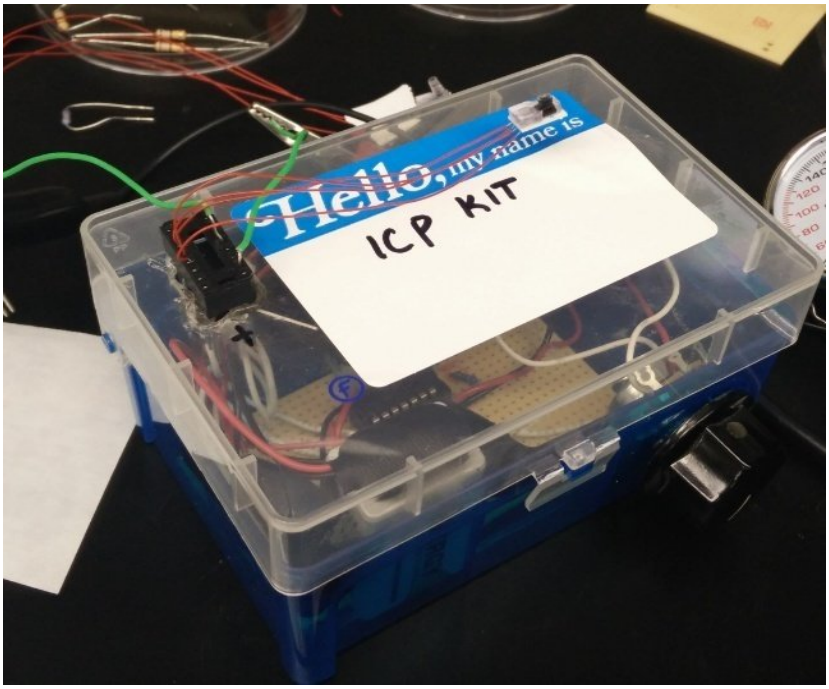

Bench Testing

Static test experimental setup

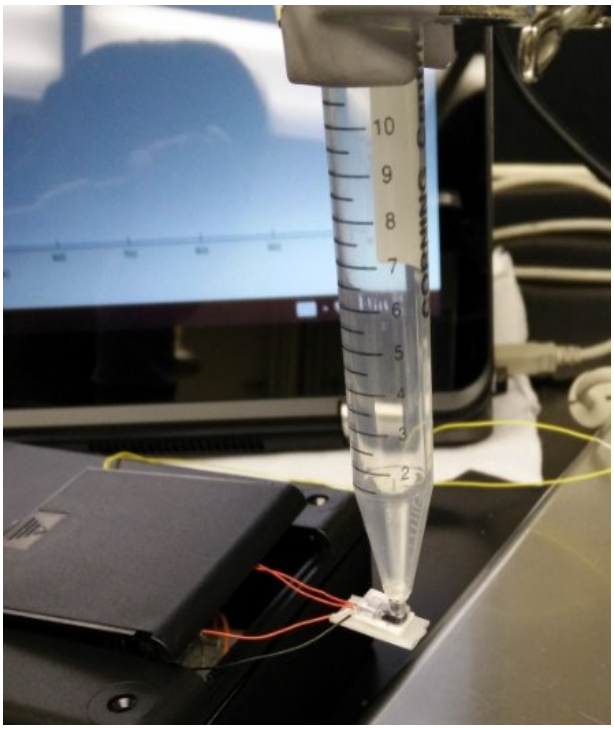

Dynamic test experimental setup

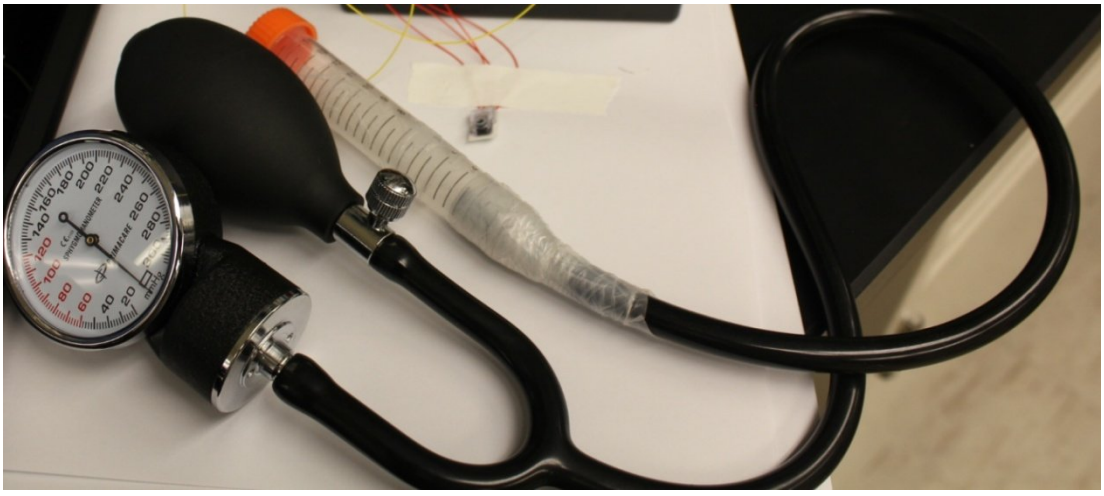

Animal Model Implementation Test setup